

RECENT IMPROVEMENTS AND FUTURE PLANS AT THE UNIVERSITY OF HAWAII
LUNAR AND SATELLITE RANGING STATION

M.L. White
Lure Observatory
Institute for Astronomy
University of Hawaii
Kula, HI 96790

Telephone (808) 878-1215
Telex 7238459

ABSTRACT

Significant improvements have been made to the University of Hawaii laser ranging station during 1986. A new data processing and software development computer has been installed, and the real-time ranging computer has been upgraded. The ranging electronics and optical systems have been improved. These improvements and future station plans are discussed in this paper.

RECENT IMPROVEMENTS AND FUTURE PLANS AT THE UNIVERSITY OF HAWAII LUNAR AND SATELLITE LASER RANGING STATION

I. Computer Hardware Improvements

During 1986 at Hawaii, major improvements have been made to the computer hardware. Due to the increased demand on the ranging computer by lunar operations, and the necessity for on site lunar data analysis, a new Micro PDP-11 computer was purchased and installed at the observatory's administrative office in Waikoa. The new computer will free up the real-time ranging computer for operations, while allowing the majority of software development and lunar data analysis to be done at Waikoa. Future lunar data analysis requires near real-time normal point formation. The operation's crew will hand carry lunar data on a removable 26 megabyte disk cartridge to the Waikoa data processing center where the Micro PDP-11 will be used to create normal points and earth rotation/polar motion solutions. The lunar data products will be entered on the G.E. Mark 111 system the morning after the data is acquired.

Concurrently, plans were developed and hardware purchased to expand the real-time operating computer backplane from 18 to 22 bits, increase the virtual memory to 1.25 megabytes and increase the data storage capacity to 52 megabytes. These changes will significantly speedup real-time execution and streamline operational procedures.

II. Optical Improvements

A new receive package was installed in the Multi-Lens-Telescope (MLT), greatly improving lunar ranging efficiency. During normal lunar operation the MLT alignment must be routinely compared to a guide camera to insure correct telescope pointing. The new receive package allows the operator to verify the telescope pointing and alignment by the electro-mechanical movement of a movie camera into the same location as the photo multiplier tube. The new receive package allows one operator to perform a task in several minutes which previously took two operators nearly 30 minutes.

The MLT has 160 individual turning mirrors which direct incoming light to a common focus. These turning mirrors were refastened after the epoxy, previously used to hold the mirrors in place, deteriorated. The deterioration of the epoxy caused the mirrors to become loose and unstable. The old epoxy was not as moisture resistant as expected. The new epoxy was applied in large quantities and is moisture resistant. A dramatic improvement in MLT alignment stability was observed as a result of applying the new epoxy. A complete MLT alignment is now required every 2 months rather than every 2 weeks.

A 1 angstrom bandpass filter was purchased and successfully tested in the lunar receiver. The double peak, polarized interference filter substantially improved the signal-to-noise ratio on illuminated lunar targets and during daylight lunar ranging.

Due to the unique design of the MLT, which consists of 80 individual light paths of varying lengths, a light pathlength compensator is needed. The compensator consists of 3 cylinders of solid glass that fit in the optical path of the MLT, delaying the longer path lengths. As is often the case with unique optical components, substantial fabrication time is required. After nearly two years since placing the order for the compensator, it is expected to be delivered by the end of 1986.

III. Ranging Machine Improvements

Plans to install a new Micro-Channel Plate (MCP) detector in the satellite and lunar systems have been approved. As part of the the MCP package, new Tennelec discriminators will replace the currently used Ortec 934 discriminators. The new detectors are likely to be installed and acceptance tested by early 1987. Other future ranging machine improvements include new 50 pico-second vernier cards for the University of Maryland event timer currently used in the lunar system.

IV. Calibration

Currently, both the the lunar and satellite calibration are accomplished by ranging to an external calibration board located approximately 1 kilometer from the station. Internal calibration will be implemented by early 1987. The satellite system internal calibration will be easily accomplished due to the uniquely, simple design of the transmit/receive optics. The lunar system however, has a separate transmit and receive telescope making internal calibration more difficult. The use of a lengthy, single mode fiber optic cable will be required, and considerable testing will be necessary to verify calibration accuracy. Unlike the satellite system which uses a single stop epoch timer, the lunar system uses a multi-channel event timer, making real-time calibration possible. In both the satellite and lunar system the external calibration board will continue to be used as a verification of the internal calibration.

V. Observing Schedule

Over the past 2 years, the Hawaii ranging station has generally scheduled 2 observing shifts, back to back during the evening, Monday through Friday. The 2 shifts range to LAGEOS and the moon with LAGEOS as the first priority. This schedule resulted in a considerable loss of lunar data when optimal ranging times occurred over the weekend, and occasional loss of LAGEOS data, when LAGEOS moved out of the night-time window. As of August 1986, the station began scheduling one shift during optimal lunar ranging periods (including weekends), and scheduling the second shift to maximize lageos coverage. This new scheduling scheme, though sometimes complicated in the case of lunar scheduling, has greatly improved lunar coverage and contributed to increased lageos tracking efficiency.

VI. Conclusion

The University of Hawaii laser ranging station has provided very consistent state-of-the-art satellite ranging measurements to the scientific community for the past six years. During the past 3 years, the station has regularly provided lunar ranging data in quantities previously unobtained, and with normal point accuracies of less than 2 centimeters. The improvements discussed in this paper will allow the station to maintain state-of-the-art status by improving the ranging system accuracy and precision by a factor of 2 to 3, providing increased satellite and lunar coverage, and providing real-time earth rotation/polar motion solutions.



THE McDONALD OBSERVATORY LASER RANGING STATION : MLRS

J.R. Wiant, P.J. Shelus
McDonald Observatory and Department of Astronomy
University of Texas at Austin
Austin, Texas 78712-1083 - USA -

Telephone (512) 471 4461
TWX 910874 1351

ABSTRACT

Since the last Workshop of this type, which had been held in England some two years ago, a number of changes have been made with respect to laser ranging operations at McDonald Observatory near Fort Davis, Texas. First and foremost is the fact that all lunar operations on the 2.7 m (107") McDonald reflector have been discontinued and our entire operations, both lunar and LAGEOS, have been totally assumed by the stand-alone, dedicated 76 cm (30") based system now known as the McDonald Laser Ranging Station, MLRS. Since the MLRS system has been the subject of many reports in the past, this paper will only summarize the up-grades and improvements which have been made to that system over the past two years. These improvements include, but are not limited to, a new high-energy, short-pulse Quantel Nd-YAG laser capable of ranging both to the moon and to LAGEOS, a second Data General NOVA-based computer and Winchester-type hard-disk system providing for improved observing capabilities as well as for data pre-processing and analysis, the installation of 21-bit encoders and a new telescope bearing for improved tracking and pointing, as well as new timing and photomultiplier equipment. All of the relevant changes will be presented and discussed together with the impact of those improvements on the MLRS data yield, both with respect to the moon and to LAGEOS.

This work is being supported by the National Aeronautics and Space Administration under Contract NAS5-29404 to McDonald Observatory and the University of Texas at Austin from the Goddard Space Flight Center in Greenbelt, Maryland.

Introduction

The McDonald Observatory and Department of Astronomy of the University of Texas at Austin continues to operate the McDonald Laser Ranging Station (MLRS) for the NASA Crustal Dynamics Program under contract to Goddard Space Flight Center. The MLRS is a dual purpose installation designed for laser ranging operations to both lunar and artificial satellite targets. The station is located on the grounds of the Observatory, about 17 miles north of Fort Davis, Texas. Various operational, programmatic, and logistical support is also provided by several personnel associated with the Department of Astronomy on campus at the University of Texas in Austin. Since the MLRS system and its operations have been the subject of so many reports in the past, this paper will only summarize the up-grades and improvements which have been made to that system over the past two years (since the last laser ranging workshop).

Hardware Changes

The 18-bit absolute encoders on both axes of the alt-alt telescope were removed and replaced with 21-bit encoders. Only minimal software changes were required to take full advantage of the increased angular resolution and the expected pointing and tracking improvement was recognized immediately. The full extent of MLRS pointing and tracking capabilities has still not been fully realized however because of suspected bearing problems (especially for the telescope yoke). Work on this sub-project continues.

A single, short-pulse, dual-power laser was supplied to us by NASA/Goddard to replace the original two-laser system of the MLRS. With the help of Grant Moule, from the Australian laser ranging station at Ororral, this new laser went from shipping crate to operational status at the MLRS within nine calendar days. The advantages of the new laser system over the old are numerous. Alignment and calibrations need now only be performed for a single laser. There is possible a very rapid changeover from lunar to LAGEOS operations and vice-versa (~20 seconds). A more convenient physical arrangement allows for easier maintenance. And, of course, the ability to range the moon with a 200 picosecond pulse (instead of the 3 nanosecond pulse of the former system) has not been lost on the LLR analysts.

The Varian "super-tube" photomultiplier was recovered from the TLRS, when that system was up-graded to a more powerful laser, and this new tube was then incorporated within the MLRS. This new PMT has been observed to reduce the RMS of both the internal calibration and the data themselves by a factor approaching two over their former values. Further, the Varian is considerably less "noisy" than the previous tube used. A cloud on the horizon is the possible contamination of data quality caused by a potential time-dependent "beam-walk" problem across the face of the tube.

In order to establish the capability of performing simultaneous data acquisition and data reduction at the MLRS, some additional funding provided to us by the U. S. Naval Observatory allowed us to purchase and install an entire second Data General Nova computer system within the MLRS operating environment. In addition to a new CPU, there were two 160 M-Byte Winchester disk systems (with associated dual-controllers), an additional 9-track magnetic tape deck, and various communications peripherals purchased. As an additional benefit of this new computer system is the fact that two data streams can be simultaneously processed (when no observing is being performed) and we can temporarily share equipment to retain full observational capability (at the expense of data reduction) if there is an equipment failure. An IBM PC/AT Microcomputer was purchased with various peripheral hardware and software items as we seek to do "smart" terminal emulation in anticipation of the eventual "death" of our old and venerable Tektronix 4025 graphics terminals. Finally, an Apple Macintosh PC microcomputer was purchased for documentation preparation, the making of schematic

drawings, monthly reporting, and direct file transfers between the Austin and the Observatory portions of this project.

In an attempt to alleviate as many seeing-related problems as possible at the MLRS, an air conditioning unit was purchased and installed in the MLRS telescope room. This unit provides active temperature and humidity control during non-operating hours. Operations have been streamlined since this installation because far less time need now be spent in waiting for the telescope to come to thermal equilibrium with its surroundings after the dome has been opened in anticipation of ranging operations.

Finally, after 15 years of faithful service, our LORAN-C receiver has been retired. Its role in providing accurate epoch monitoring at the station has been taken over by a Global Positioning System (GPS) receiver. Also, we have abandoned our attempts to incorporate the computer controlled narrow-pulse filter in the MLRS receive system.

Software and Logistical Changes

As might be expected, a myriad of software changes were incorporated into the MLRS computing systems in concert with most of the hardware changes mentioned above. Fortunately, because the MLRS was originally designed to be a software intensive one, these software changes could be designed, coded, and debugged "off-line", well before the implementation of the actual hardware changes. Thus, in most instances, they could be incorporated into the system without requiring additional station down-time except for that which was required for the actual hardware changes themselves. Further, many routine changes were made in the data processing systems to accommodate data format and electronic communications up-dates and up-grades. Again, each of these was completed and implemented with a minimum of difficulty, all the time maintaining active communications with the outside world.

As far as MLRS observing operations go, it is safe to say that since December 1985, the station has finally realized a large percentage of its original observational potential. Day-time LAGEOS ranging is now accomplished with the same ease as night-time ranging and the lunar system has become as reliable as the 2.7-m system was. In reality, over the past year or so, only the weather has been our major problem (see the illustration of MLRS data statistics for both the moon and LAGEOS). With that in mind, a great deal of time and effort has been expended to examine the trade-offs between cost and data throughput to provide for the most cost effective operation of the dual lunar and artificial satellite capabilities of the MLRS. To that end we have strongly recommended that a minimum of two-shift operation always be present at a dual-capable station like the MLRS. In that scenario, one of the shifts is relatively fixed in an eight hour per day, five day per week schedule to concentrate on the LAGEOS target. The second shift is quite variable and "chases the moon" as efficiently as possible, in concert with whatever physical and personnel constraints may exist. Each shift, wherever possible, attempts to take the other crew's target as a "target of opportunity". To the best of our ability and within the constraints of our budget, those are the procedures which we try to emulate at the MLRS.

Using this scenario for our observing operations, it is easy to see that the scheduling of the LAGEOS crew is quite straightforward and can be implemented with little difficulty. For maximum lunar data throughput things get a bit more difficult. We attempt to maximize our coverage at the lunar quarters (completely ignoring week-ends). During a lunar ranging session we attempt to obtain a minimum of three Apollo 15 reflector observations with as wide an hour angle spread as possible; all remaining time is spent on observing the other three accessible lunar targets and/or observing any potential LAGEOS "targets of opportunity". At the present time, a successful lunar observation is considered to be made when a total of 25 photon returns have been identified (in real-time) by the observing crew.

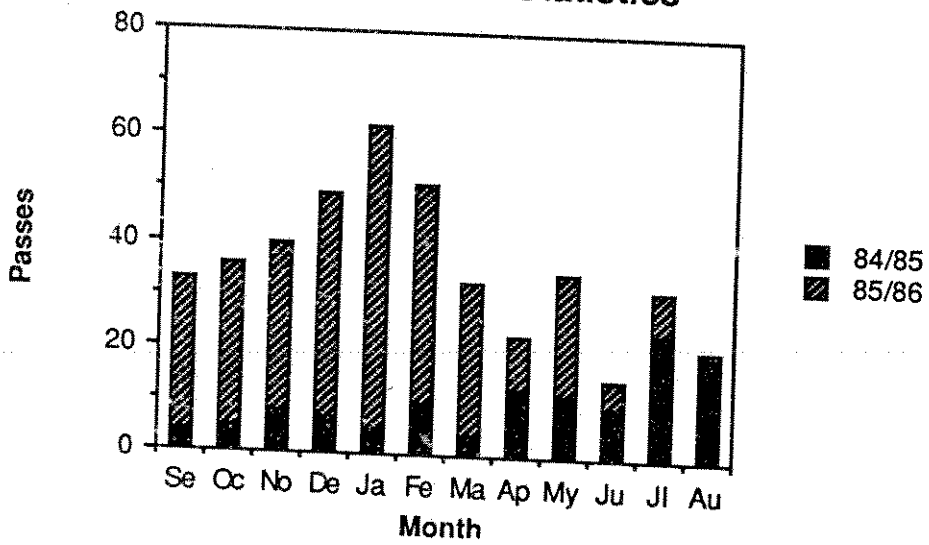
On other matters, as reported elsewhere in these workshop proceedings, we have established real-time Earth orientation computations at the MLRS, using lunar data. Normal lunar laser ranging data is identified, filtered, compressed, formatted, and analyzed on-site, and when sufficient data exists, an Earth orientation reduction is performed. The results are electronically transmitted to the U. S. Naval Observatory (and to other interested parties), usually within hours of the data taking.

Finally, the MLRS Operational Readiness Review was satisfactorily completed in the summer of 1985, testifying to the fact that the MLRS has indeed taken its place in the world among the other fine stations in the international laser ranging network. The road to the completion of the MLRS was a long and a hard one and, at times, many of us had our doubts as to whether or not it would ever come up to the standards which were set by our old 2.7-m system. To the future, we look forward to the time when the MLRS might be moved from its present "saddle-site" to one which is much more favorable, in order that it might be truly raised to its full observational potential.

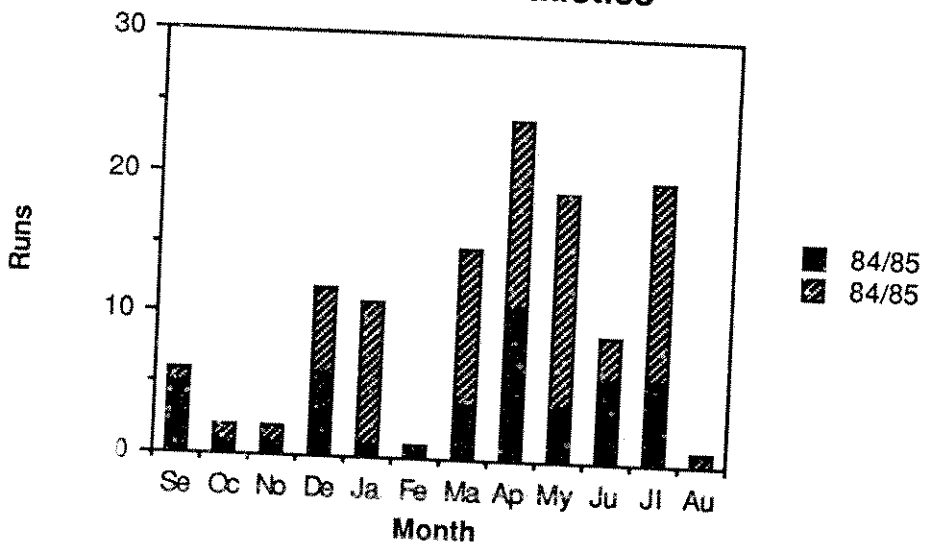
Acknowledgements

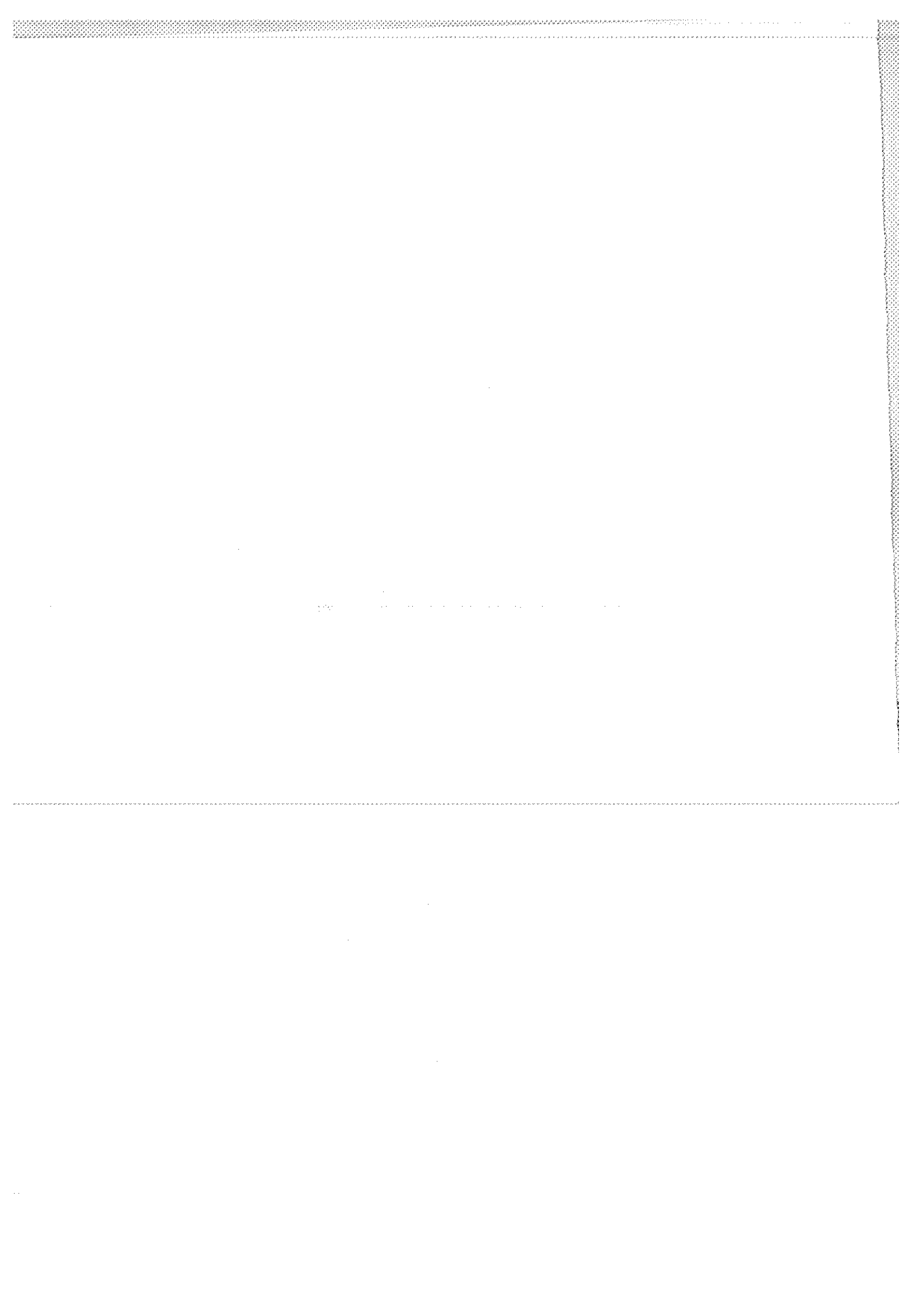
The authors acknowledge that this work is being supported at McDonald Observatory and the University of Texas at Austin by National Aeronautics and Space Administration Contract NAS5-29404 out of Goddard Space Flight Center, Technical Officer Mr. Robert L. Appler.

MLRS/LAGEOS Statistics



MLRS/Lunar Statistics





START DETECTOR FOR THE MODE LOCKED TRAIN LASER RADAR

I. Prochazka
Czech Technical University
Faculty of Nuclear Science and Physical Eng.
Brehova 7, 115 19 Prague - Czechoslovakia -

Telephone 848 840
TWX 121254 FJFI C

ABSTRACT

The start detector + discriminator for the mode locked train laser radar is described. The device is based on the semiconductor optical switch. The jitter test experiment using streak camera and the optical sampling application of the detector is described.

START DETECTOR FOR THE MODE LOCKED TRAIN LASER RADAR

I. Procházka

The Interkosmos laser radar is using the mode locked train transmitter since 1983 /1/. The laser emits the train of pulses HAFWK30psec, spaced at 2.00 nanoseconds (see fig.1). To start the ranging electronics channel, the appropriate detector/discriminator capable of responding to the train of pulses was to be developed. The most common set up consisting of fast photodiode followed by constant fraction discriminator is far from optimum, because no discriminator available is able to respond to a single pulse from a narrow spacing train with low jitter. A special type of a fast fixed threshold detector/discriminator was developed by Cech /2/ and applied 1983-85. It was based on the fast photodiode followed by tunnel diode monostable circuit and pulse forming circuit. The jitter and time walk 150psec at the dynamical range 1:2 was achieved. To meet the high requirements of picosecond ranging using the train, the new principle of detector/discriminator was developed.

Its electrical scheme is on fig.2. The circuit is based on the in house built semiconductor opto switch (OS). The switch is working in the avalanche regime generating on its output the uniform signal (see fig.3) of several volts with fast leading edge 10mV/picosec. The OS switches at the fixed signal level, thus the first pulse higher than this level is causing generation of the electrical output pulse. Taking into account the pulse duration <30psec, the fixed threshold discriminator technique is no drawback for the application.

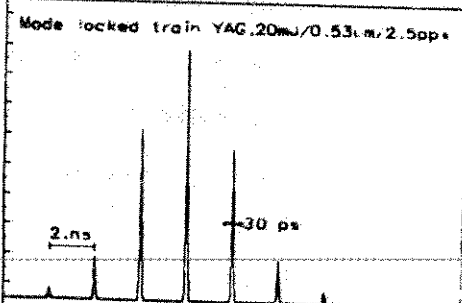
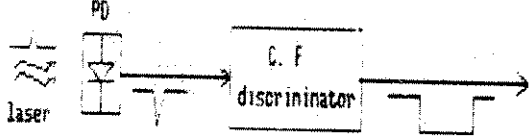
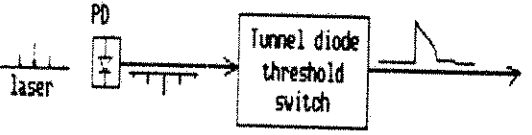
The jitter of the device was tested and the circuit optimised using the train of 10-30psec laser pulses and a streak camera (Hamamatsu 979) as a detector. The camera was triggered by the circuit output, the laser pulse was displayed. The digitised data from the camera were processed in the on line computer. The jitter of the device may be determined from fluctuations of the pulse position on the streak screen taking into account the trigger jitter of the camera itself (18psec measured by the manufacturer). On fig.5 there is a plot of consequent streak records. The excellent overlap of the pulses/trains may be seen. Using a streak camera, the jitter ranging 10-40picosecond was measured. The actual value of the jitter depends on the laser pulse length and amplitude fluctuations. Using pulses longer than 50picoseconds, the trigger jitter was about 0.4 times the pulse length.

Using two identical circuits set to different trigger levels and a high resolution time interval meter, the simple sampling scheme may be constructed. One detector starts the counter the second it stops. On fig. 6 there is a histogram of measured times. The peaks separation corresponds to the laser resonator round trip, the peaks width determines the jitter ($2 \times \text{Start} + \text{counter}$) typ. 50-70psec. The quality of mode locking may be estimated from the background. For comparison, on fig.7 there is the analogical histogram of measurements taken on the passively

mode locked laser oscillator incorrectly adjusted, transmitting multiple pulses. The laser output was monitored simultaneously on the streak camera. The background is of order higher. Thus, the pair of the START circuits may be used for quick check of the mode locked train transmitter in the quasi sampling mode with effective bandwidth of 5GHz. The possibility to monitor the mode locking quality is attractive especially in connection with passively mode locked laser for picosecond pulses generation.

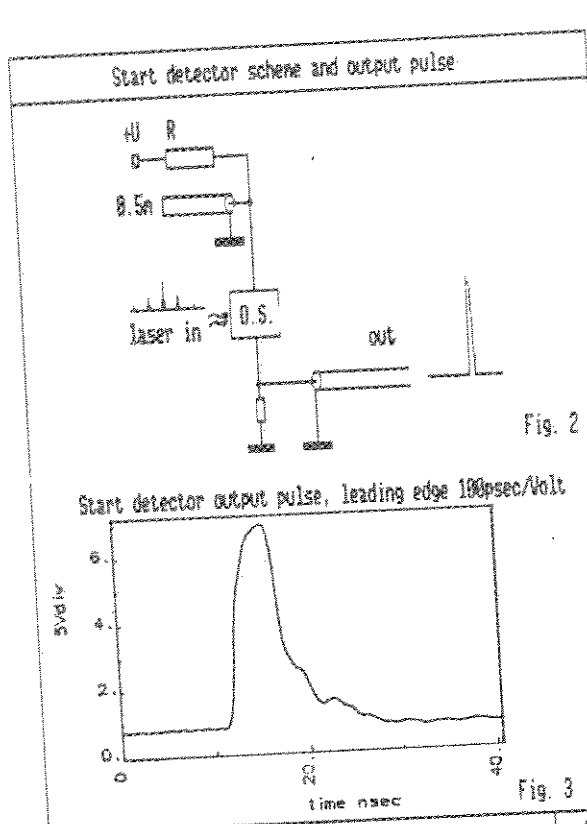
Literature

- 1/ K.Hamal et all, Interkosmos laser radar, version mode locked train proceedings of 5-WLRI, Herstmonceux, Sept. 1984, edited by J.Gaignebet
- 2/ M.Cech, Start discriminator for the mode locked train laser, in /1/

Start detector requirements	Available start detector/discriminator schemes
<p>SLR Transmitter output pulse</p>  <p>Mode locked train YAG, 20mw/0.53um, 2.5pps</p> <p>2 ns</p> <p>30 ps</p> <p>Fig. 1</p>	<p>1/ Standard scheme :</p>  <p>- not applicable for mode locked train of pulses with nsec spacing because of C.F. discriminator time response</p>
<p>Requirements:</p> <ul style="list-style-type: none"> - process train of psec pulses with few (1..6)nsec spacing - low jitter (50 psec - dynamical range) 10 : 1 - rugged and simple - simple adjustment/test procedures 	<p>2/ Scheme by M.Cech (5-th WLRI, Herstmonceux, 1984)</p>  <ul style="list-style-type: none"> - applied in Helwan, 1983..1985 nissions - jitter/time walk 150 psec / dyn.ratio 2:1 only - delicate set up
<p>I.Prochazka Start Detector For Mode Locked Train Laser Radar</p>	<p>I.Prochazka Start Detector For Mode Locked Train Laser Radar</p>

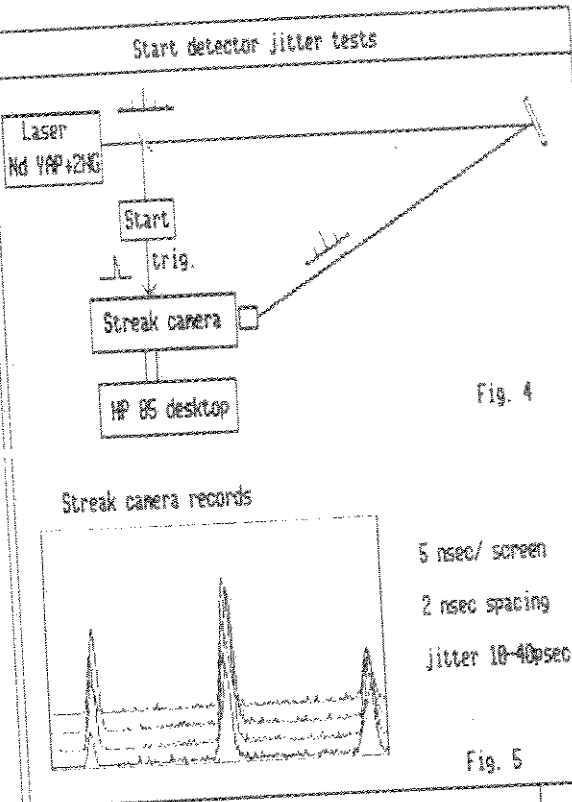
1

2



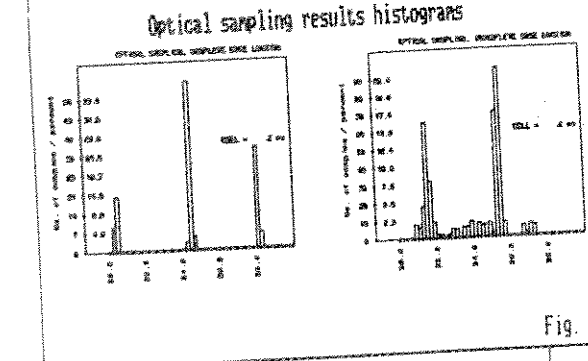
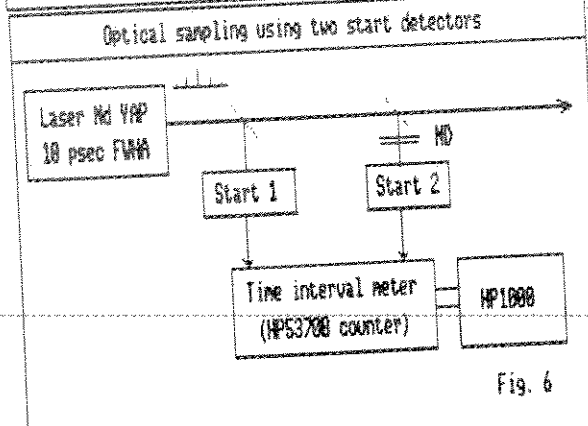
I. Prochazka
Start Detector For Mode Locked Train Laser Radar

3



I. Prochazka
Start Detector For Mode Locked Train Laser Radar

4



I. Prochazka
Start Detector For Mode Locked Train Laser Radar

5

Start detector summary

Start detector/discriminator performance:

- process train of picosecond ML pulses with nsec spacing
- fast fixed threshold discrimination
- uniform, high amplitude output
- internal delay (1 nsec)
- jitter (40 psec)
- dynamic range) 20 : 1
- optical sampling capability :
 - * passive mode locking check
 - * equivalent bandwidth 5 GHz
- changing bias voltage, serves as a laser monitoring PD
- applied in Helwan 1986,
 - calibration ranging jitter before 520ps after 300 ps
 - system stability before 150ps after 120 ps

I. Prochazka
Start Detector For Mode Locked Train Laser Radar

6

AMBIGUITY AND RESOLUTION OF A MODE-LOCKED
PULSE TRAIN LASER RADAR

R. Neubert, B. Ritschel, L. Grunwaldt
Academy of Sciences of G.D.R.
Central Institute for Physics of the Earth
Telegrafenberg A 17, Postdam 1500 - G.D.R. -

Telephone
Telex 15305

ABSTRACT

The accuracy of a multipulse laser radar has been studied with indoor experiments and computer simulation. For the experiments a mode-locked Nd-YAG laser producing 7 to 9 pulses of 4.6 ns spacing at 10 Hz repetition rate is used. The frequency-doubled pulses are divided by a beamsplitter and recombined at the photomultiplier which is working at the single photoelectron level. The time-of-flight data are treated by cross-correlating the empirical distributions corresponding to the two light paths. This leads to an estimate of the time-of-flight difference. Using a large amount of data sets the following parameters are determined :

- a) The percentage of estimates shifted by more than half a pulse spacing.
- b) The standard deviation of the unshifted estimates.

For the parameters of our system, the percentage of "good" estimates is higher than 90 % if more than 200 measurements are used. A standard deviation of about 100 ps is obtained under the same conditions. These results are obtained using electrostatic PMT's with about 500 ps jitter. Good agreement between the experiments and computer simulations is found. Thus the simulation method is used to determine the system performance in a wider parameter range.

The use of the full mode-locked pulse train for laser radar is advantageous because of laser simplicity and efficient use of its energy. However, because of the ambiguity problem, this concept found only limited applications as yet [1], [2]. The ambiguity of such a laser was discussed in an earlier paper [3] on the basis of computer simulation. In the following we report on comparison of the simulation results with laboratory experiments.

Experimental setup

The simplified optical diagram of the setup is shown in Fig. 1. The signal of the mode-locked Nd-YAG laser is split into three parts. A first part is reflected by a beam splitter (BS) to a silicon photodiode (PD) which is connected to the start input of the PS-500 time interval counter via a leading edge trigger. The stop receiver (usually a PMT) is illuminated with very weak signals reaching it along two different ray paths:

- the short calibration path 1
- the longer ranging path 2

The attenuation to the single-photoelectron level is achieved by neutral density filters (F). By choice of the filters, the signal level is adjusted in such a way, that 10 to 50% of the laser shots are causing the emission of one electron from the PMT photocathode. Thus, the stop of the counter occurs randomly by a photon arriving along path 1 or path 2. The single-photoelectron pulses from the PMT are detected by a constant-fraction discriminator [4] to reduce the timing noise caused by PMT gain fluctuations.

The main specifications of the passively mode-locked Nd-YAG laser, which has been designed in our laboratory, are given in Table 1.

Table 1: Specifications of the Nd-YAG laser

Energy of pulse train ($\lambda = 1.06 \mu\text{m}$)	3 mJ
Number of pulses per train	7-9
Pulse separation	4.6 ns
Pulse width	68 ps *)
Repetition rate	10 Hz
Laser rod dimensions	5 x 75 mm
Optical resonator type	large radius mirrors
Resonator length	69 cm
Modelocker	Soviet dyes 3955 or 3274 in methanol

*) Average value for $\lambda = 1.06 \mu\text{m}$, estimated by the two-photon fluorescence method

For second harmonic generation, a KDP crystal is used. To

have definite polarization of the laser, Brewster plates are introduced into the optical resonator.

Time resolution tests

Starting point for the analysis of the measurements is the frequency distribution (histogram) of the time-of-flight values. This distribution is calculated usually from 1000 measurements. A typical example is shown in Fig.2. To determine the resolution of the system, the part of the distribution corresponding to one ray path is necessary only. As an example the left-hand part of Fig.2 is plotted in Fig.3 with higher resolution of the abscissa. The pulse structure of the laser is well resolved, but to take into account the partial overlap of the individual pulses, the distribution is analyzed using a least-square fit of a sum of Gaussian functions. To reduce the number of free parameters, the separation and width of the peaks have been assumed to be equal. The RMS width of the peaks obtained in this way can be used as a measure of the overall time resolution. The most important contribution to the timing noise is the fluctuation of the PMT delay (jitter). This quantity depends on PMT type and sample and its working conditions (voltage divider, illuminated area). Some contributions are also given by the amplitude fluctuations. This effect depends on the discriminator performance. Some results of resolution tests for different PMT tubes obtained in earlier experiments are shown in Table 2.

Table 2: Time resolution of the system

PMT type	Sample No.	RMS - Jitter (ps) *)	
		No diaphragm	1 mm diaphragm
RCA C 31034A	47105	540	370
FEU 79	4665	530	530
FEU 136	2053	600	470

*) Overall jitter including start, i.e. no deconvolution applied. Start photodiode type SP 109 directly connected to the counter (HP 5370 in these experiments).

It can be seen that the restriction of the illuminated area has some effect on the resolution, especially for the RCA C 31034A tested. The best resolution was obtained with this tube as yet, but with selected samples of other electrostatic PMT even better results might be attained. To determine the contribution of the start-time noise, some experiments were carried out using a silicon photodiode for the stop too. Using the HP 5082-4220 type in both channels, a RMS resolution of 300 ps was obtained. This value could be improved to 150-200 ps using the fast SP 109 photodiode (VEB Werk fuer

Fernsehelektronik Berlin). Assuming that the start- and stop-time fluctuations are equal and independent in this case, the RMS start-time noise can be calculated to be 100-140 ps. For the experiments with PMT receiver, the SP 109 was always used. Thus, the jitter of the RCA C 31034A can be estimated by quadratic subtraction of the start noise to be around 350 ps. From this example it can be seen, that the start-time noise has only small influence on the overall resolution in our experiments.

The precision of the cross-correlation method

The generally adopted method for treating the data of a mode-locked train laser radar is to calculate first the frequency distributions of the calibration- and the ranging-measurements separately, and then to determine the time shift for maximum correlation of the two distributions. An example distribution is shown in Fig.2. The two subdistributions according to path 1 and 2 are well separated from each other by roughly 60 ns. Convoluting both distributions, Fig.4 was obtained. In this figure the convolution sum is plotted like a polygon linking the points separated by the bin width of 250 ps. The maximum can be determined very accurately using some interpolation method. In our case we obtain for the time shift of maximum correlation (61.16 ± 0.1) ns.

To investigate the precision of the method, the measurements of this and several other experiments were arranged into groups. Then the cross-correlation method was applied to each group so that an ensemble of time shifts is obtained from which statistical estimates for the precision can be gained. The parameters under consideration are:

1. the percentage of time shift results deviating from the real value not more than half a pulse separation (this quantity called "uniqueness")
2. the RMS error of the results deviating not more than half a pulse separation

These parameters are plotted in Fig. 5 and 6 in dependence of the quantity of measurements. As a normalized measure of the data quantity we are using $(1/n_1 + 1/n_2)^{1/2}$, where n_1 and n_2 are the number of measurements for path 1 and path 2, respectively. This is just the probable error of the ranging average for a single pulse system, expressed in terms of the standard deviation of a single time interval measurement. To estimate the uniqueness (resp. ambiguity) and precision from the measurements, 10 runs of 1000 points each are used. The total ensemble of 10000 measurements is arranged into groups of $n_1 + n_2 = 60, 120, 240, 480$ individual measurements. For each group the cross-correlation method is applied resulting in the generation of an ensemble of ranges from which the interesting average parameters are estimated. The return rates for the two light paths are slightly changing

from run to run. Therefore averages for the parameter $(1/n_1 + 1/n_2)^{1/2}$ have to be determined also. The resulting experimental values for the uniqueness and precision are plotted with the symbol "+" in Fig. 5 and 6.

For comparison with theoretical values and to obtain more general results (including different shapes of the laser signal like reduced pulse numbers), computer simulations were carried out assuming the photodetection process to be described by Poisson statistics and the timing jitter to have a Gaussian distribution. The simulator is a pseudo random number generator which outputs two possible numbers: 0 (corresponding to no detection) and 1 (detection). The probabilities of the two states are determined by the average number of photoelectrons (s) of the pulse according to:

$$P(0) = \exp(-s); \quad P(1) = 1 - \exp(-s)$$

The simulator is called for each consecutive pulse of the group using the pulse intensities as input parameters. When the first positive answer occurs, the corresponding pulse number is stored together with some added Gaussian timing noise. By repeating this process, 5000 simulated time intervals for both the calibration and the ranging channel are generated and stored into the memory. In this process, the average return rate for the calibration is set to be 50% and for the other channel 25%.

To estimate now the performance parameters of the system in dependence on the amount of measurements, example realizations are selected from simulated measurements and then treated by the cross-correlation method in the same way as is done with the real measurements.

The selection of the individual values from the memory is done by calling an equally distributed pseudo random number generator to determine the addresses. 500 example realizations are used to estimate the performance parameters, i.e. the uniqueness and the RMS error of a cross-correlation result.

To compare the experimental values with the simulations, the average shape of the time interval histogram is needed. It has been approximated by 9 Gaussian peaks with Gaussian envelope according to

$$h = a_0 \sum_{k=1}^9 \exp(-k^2/U) \cdot \exp(-((t - t_k)^2 / 2\sigma^2)) \quad (1)$$

The average experimental parameters are $U = 4.61$, $\sigma = 386$ ps. The separation of consecutive pulses is

$$\Delta t = t_{k+1} - t_k = 4.55 \text{ ns.}$$

So the relative resolution is $C = \sigma / \Delta t = 0.0848$. Using these parameters the results marked in Fig. 5 and 6 by "*" are generated. They agree reasonably well with the experimental points, especially for the uniqueness (Fig.5). This

agreement is somewhat surprising because the laser pulse shape fluctuations are not directly modelled in the simulations. Instead, the pulse shape is chosen in agreement with the observed histograms. Note further that the simulated results showed almost no dependence from n_1 / n_2 if the above introduced parameter $(1/n_1 + 1/n_2)^{1/2}$ is kept constant. This is proved in the range $n_1/n_2 = 1...10$. For the conditions used in our experiments, the following conclusions can be drawn:

- the performance of the system can be reasonably well determined by the described simulation method
- 200 measurements for both calibration and ranging are required to have 90 per cent probability of correct assignment of the data (not shifted by a multiple of the pulse separation)
- the standard deviation of a result generated from 200 measurements is in the order of 100 ps.

The good representation of the experiments by the simulation encouraged us to study the dependence of the system performance from the laser pulse shape and the timing resolution more detailed. Some of the results are graphically represented in Fig.7 and 8. In these figures, both the uniqueness parameter (broken lines, 1 at the vertical scale corresponds to 100%) and the ratio of the RMS error of the cross-correlation result to the single-shot timing jitter (full lines) are plotted in dependence on the amount of measurements. The relative RMS error as defined describes the effect of averaging.

In Fig.7 for a fixed laser pulse shape the influence of the timing resolution is represented. As a measure of the resolution, the parameter C (defined as the ratio of the overall RMS jitter of the timing system to the pulse separation of the laser pulses) is used. The time resolution is visualized by the probability distributions of the time intervals, i.e. the shapes of the histograms for very large amounts of measurements.

As can be seen from Fig.7, the timing resolution has a very small influence on the uniqueness (resp. ambiguity) but some effect on the relative RMS error. This behaviour is to be expected. We conclude from Fig.7 that the resolution parameter C should be smaller than 0.2. Note that for a given resolution of the timing system, the parameter C can be adjusted by the separation of the laser pulses which is possible by choosing the laser resonator length.

The number of pulses in a laser pulse group is represented by the parameter U. More precisely, this is the overall width of the probability distribution of the time intervals according to equ.(1). The parameter U is chosen to be $U = 6$ in Fig.7.

The dependence of the system performance on the parameter U

for a fixed resolution ($C = 0.1$) is shown in Fig.8. As expected, the parameter U has almost no effect on the error, but strong influence on the ambiguity. Fig.8 may be used to determine the amount of data to reach a given uniqueness level. A uniqueness of 90% in connection with $U = 2$ is reached for $n_1 = n_2 \approx 50$. For $U = 1$ only 20 measurements are needed in both channels to reach 90% uniqueness. There are some methods to minimize the parameter U including laser design, the combined use of nonlinear optical effects and well matched start detectors. With generally available technology, $U = 1..2$ should be a realistic value.

Conclusion

From the results of this study we conclude that the mode-locked train laser radar remains to be an attractive variant. Its main limitation, the ambiguity, can be reasonably overcome using a sufficient data quantity. The minimum data amount for a given probability of correct assignment can be gained from this paper. As a guide to good performance, one should restrict the number of pulses per group to a minimum and adjust the pulse separation to roughly 10 times the timing jitter. A special advantage of the rigorous use of single photoelectron detection is the low level of systematic errors. This gives the possibility to attain normal point errors near 1 cm even by using conventional electrostatic photomultiplier tubes.

REFERENCES

- [1] Silverberg, E.C.: The Feedback Calibration of the TLRs Ranging System
Proc. 4th Intern. Workshop on Laser Ranging Instr.,
Austin 1981
Edt. P. Wilson, Bonn 1982, p. 331-37
- [2] Hamai, K. et al.: INTERKOSMOS Laser Radar, Version Mode-
Locked Train
Proc. 5th Intern. Workshop on Laser Ranging Instr., vol.II
Herstmonceux 1984
Edt. J. Gaignebet, Bonn 1985, p. 214-18
- [3] Neubert, R.: Simulation Studies on the Statistics of a
Multipulse Laser Radar Working at the Single Photoelec-
tron Level
Nabl. Isk. Sput. Zemli, Prague 23 (1984), p.93-102
- [4] Fischer, H.: Empfangsdiskriminator fuer Satellitenentfer-
nungsmessung mit verbessertem Zeitverhalten
Radio Fernsehen Elektronik, Berlin 31 (1982) 8, p.491-92

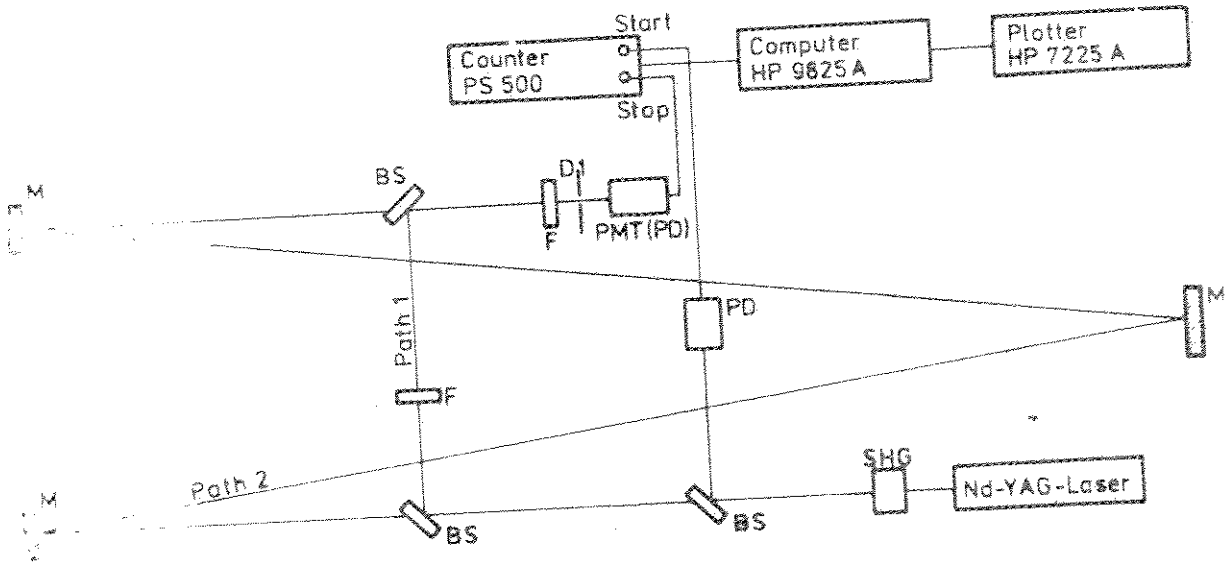


Fig. 1: Scheme of the experimental setup

BS - beam splitter, D - diaphragm
 F - neutral density filter, M - mirror
 PD - photo diode

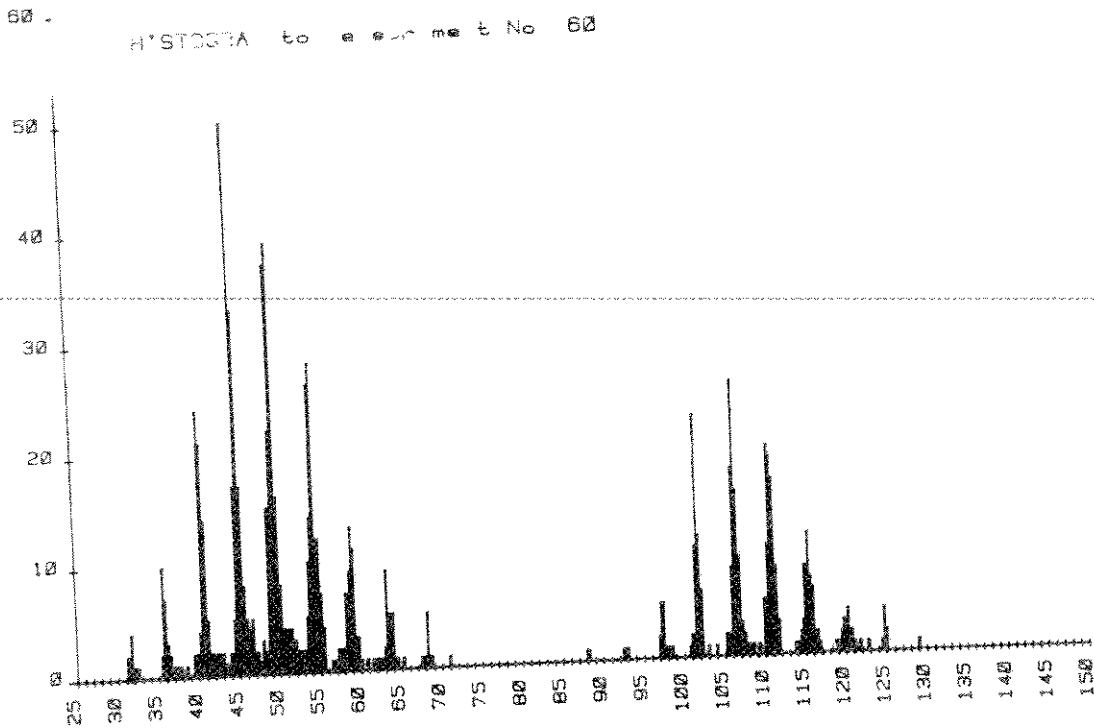


Fig. 2: Histogram of the time of flight values for a typical ranging experiment
 Abscissa: Time interval in ns
 ordinate: Number of measurements

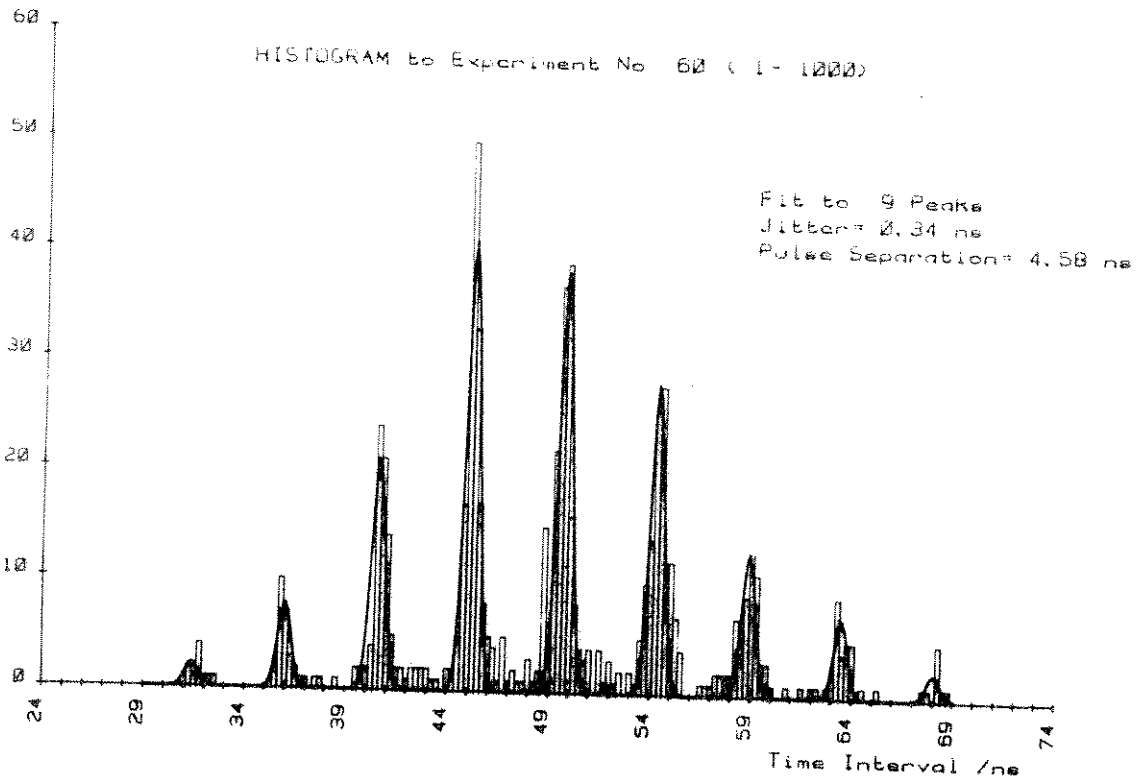


Fig. 3: Least square fit of a sum of Gaussian functions to the calibration part of experiment No. 60 (Fig. 2) bin width: 0.25 ns, RMS resolution: 0.34 ns, peak separation: 4.58 ns

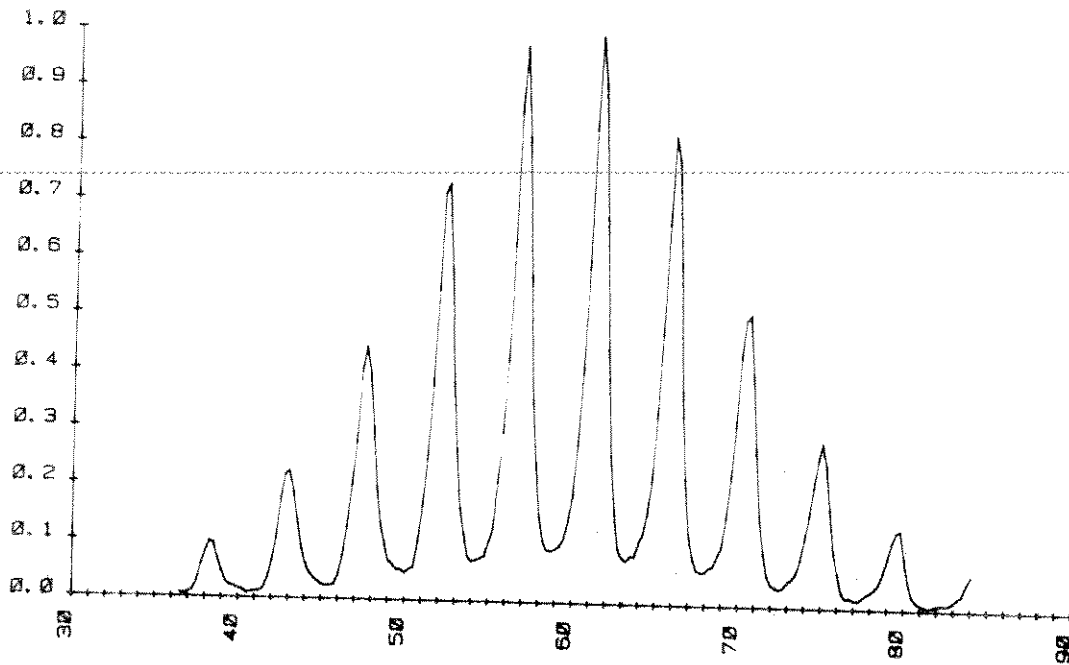


Fig. 4: Empirical cross-correlation to experiment No. 60 (convolution sum of the histograms corresponding to ray path 1 and 2 resp.)

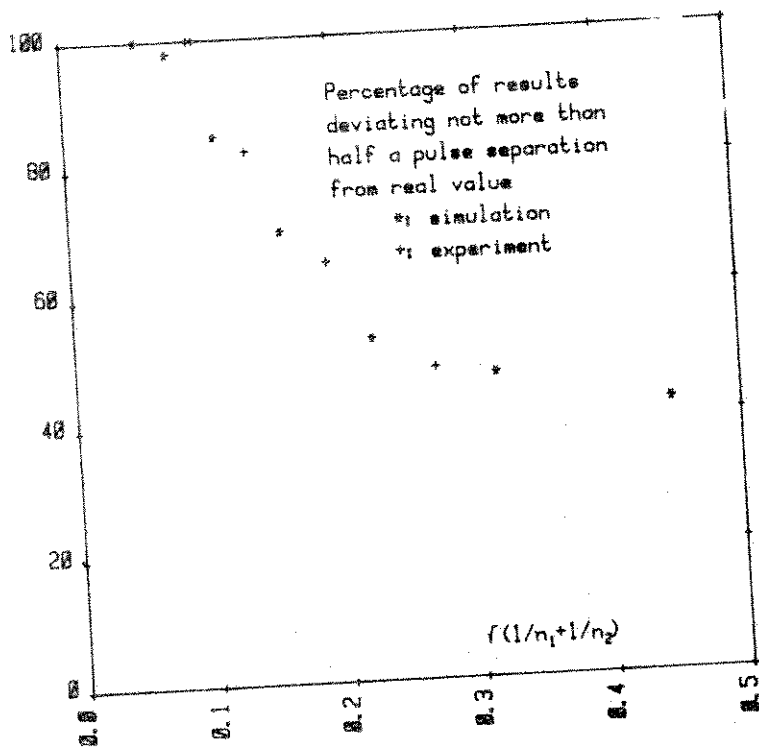


Fig. 5: Uniqueness in dependence of the amount of measurements: comparison of experiment and simulation.
 n_1 - number of measurements for path 1
 n_2 - number of measurements for path 2

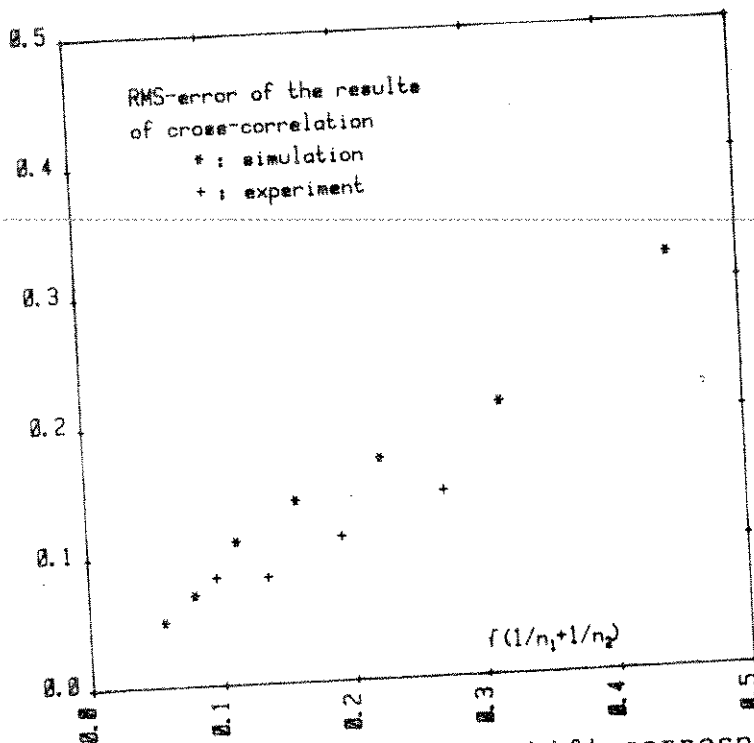


Fig. 6: RMS-error of the time shift corresponding to maximum cross-correlation: comparison of experiment and simulation

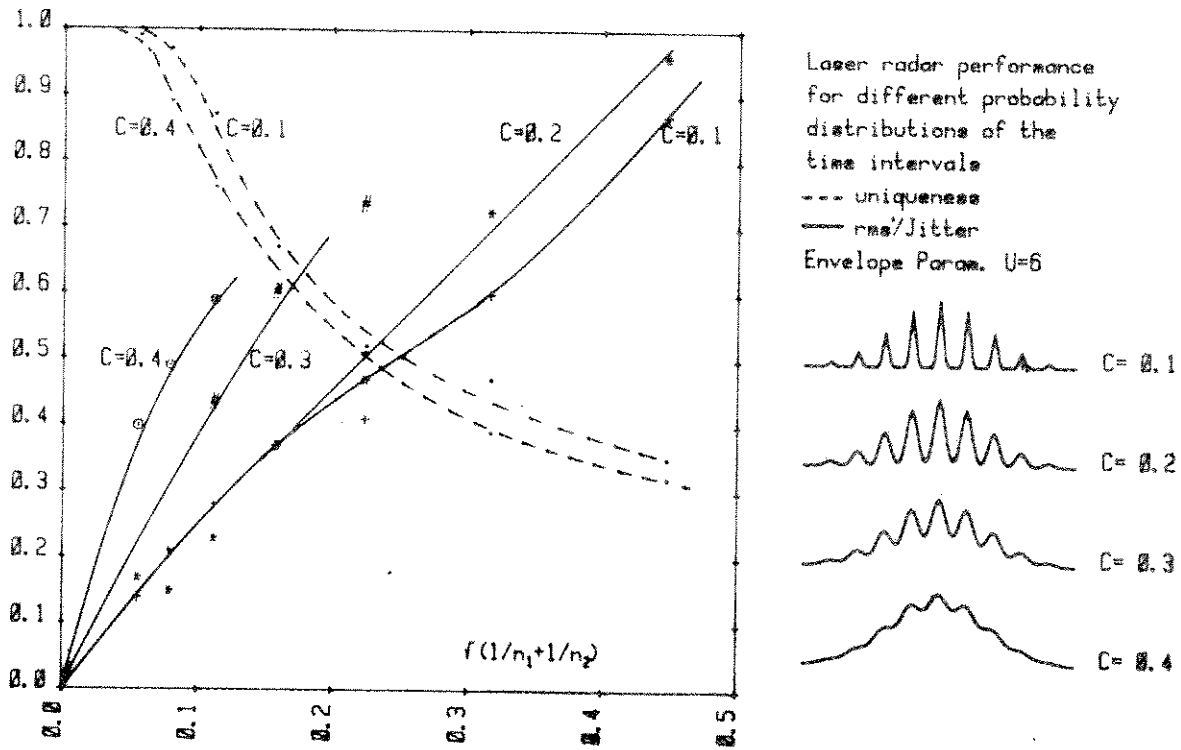


Fig. 7: Uniqueness and error obtained from simulations: dependence from timing resolution

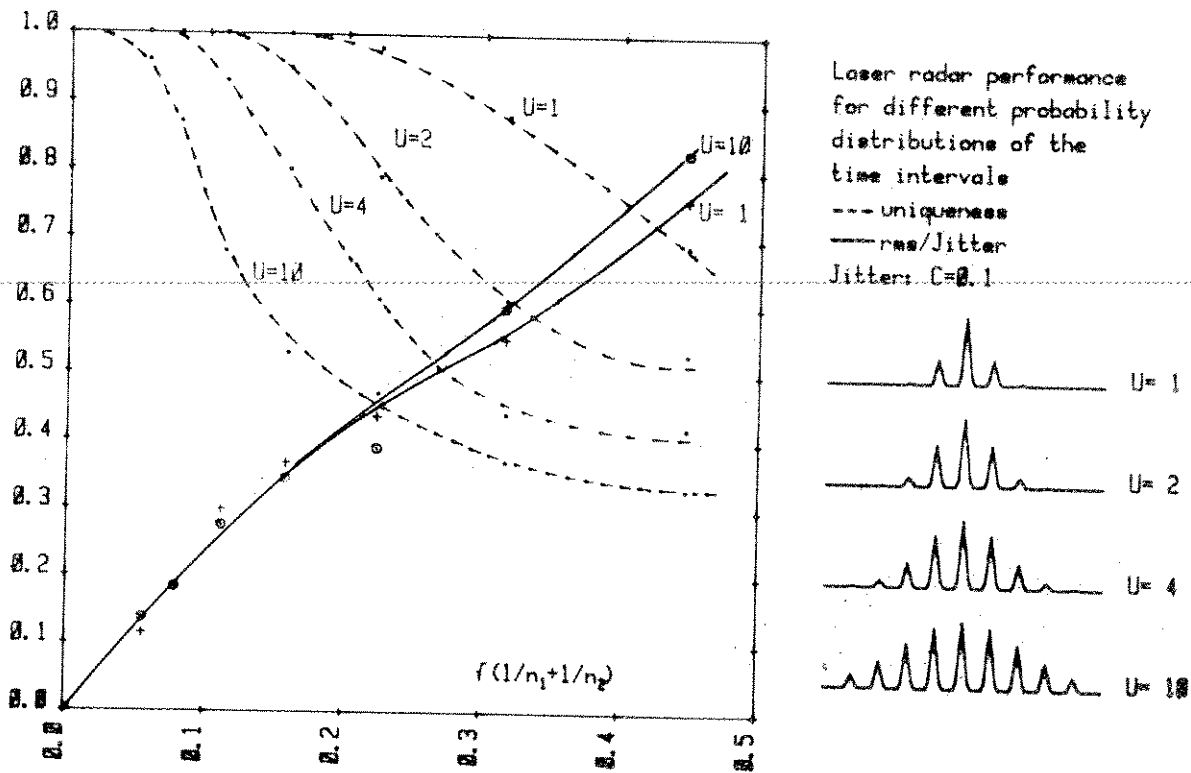
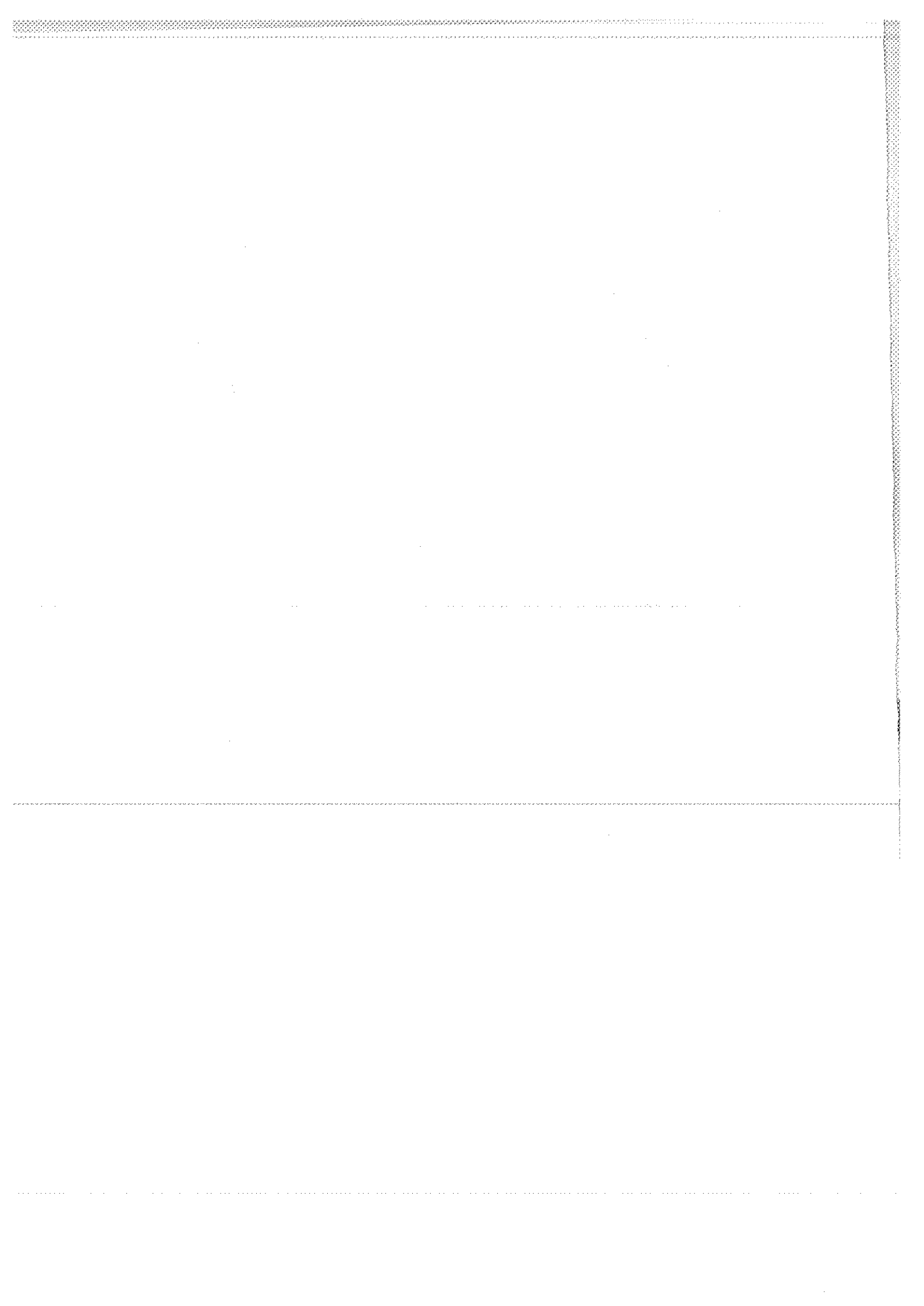


Fig. 8: Uniqueness and error obtained from simulations: dependence from the number of peaks



MICROCHANNEL/DYNODE PHOTOMULTIPLIERS COMPARISON EXPERIMENT

I. Prochazka, K. Hamal
Czech Technical University
Faculty of Nuclear Science and Physical Eng.
Brehova 7, 115 19 Prague - Czechoslovakia -

Telephone 848840
TWX 121254 FJFI C

J. Gaignebet
C.E.R.G.A.
Avenue Nicolas Copernic
06130 Grasse - France -

Telephone 93 36 58 49
Telex 470865 CERGA F

ABSTRACT

The calibration/comparison experiment for PMTs jitter measurement is described. The Transient digitizer interfaced to a minicomputer together with the powerful software package is used as a high performance discriminator and time interval meter with jitter typ. 23 psec. The transit time jitter and time walk for single PE and multi PE response of the MCP PMT Varian and dynode P11T RCA 8852 were measured.

MICROCHANNEL/DYNODE PHOTOMULTIPLIER COMPARISON EXPERIMENT

I. Procházka, K. Hamal, J. Gaignebet

Analysing the 2G or 3G laser ranging system jitter budget one may conclude, that the photomultiplier contribution is the most significant. The transit time jitter and the time walk (transit time versus amplitude dependence) are the dominant parameters. The goal of this work was to measure the transit time jitter and the time walk of the microchannel and the dynode PMT. Although these parameters have been measured by several authors before (1/,/2/ and others), the discrepancies between them and between the experience from the field was existing. That is why this measurement/comparison experiment was carried out.

The experimental set up is on fig. 1. The single pulse from Nd YAG, frequency doubled laser, FWHM of 90psec is illuminating the fast vacuum photodiode and /after an appropriate attenuation/ the PMT photocathode. To reduce the effect of transit time dependence on the illumination spot position /1/, the light spot size on the dynode PMT photocathode was reduced to 3mm. Using the ND filters, the PMT input signal was set to 1 to 50 photoelectrons. The outputs of the photodiode and the PMT were added and fed to the Transient digitizer Y-input. The optional amplifier 1000MHz/30dB was used for MCP photomultiplier at low signals. The Transient digitizer Tektronix, bandwidth 400MHz, min. 10mV/div, 512x512 pixels array is interfaced to the HP1000 computer system. The Transient together with the computer hardware/software package are used as an high performance discriminator and short intervals meter. The recording speed exceeds 10frames per second. The records are off-line processed and data analysed. The example of the Transient output is on fig. 2. The first pulse corresponds to the photodiode, the second to the PMT output. The PMT output pulse amplitude A_2 and the pulses mutual distance T are the main process output parameters. The fluctuation of T is caused by the Transient, photodiode and PMT jitters. The Transient and photodiode jitter contributions were calibrated /3/ and found to be 23psec. The constant fraction (1/2) discriminator (software modelled) was used for all the measurements.

The examples of the records are on the figures 3 to 6 for the microchannel and dynode and multi PE and low signal, respectively. The results are plotted on fig.7 and 8 where is a graph of a photomultiplier transit time difference as a function of signal strength. The vertical bars represent the jitter for given signal strength.

Literature:

- 1/ S.K.Poultney, Single photon detection and timing, experiments and techniques, Advanced electronics and electron physics, Vol.31, 1972
- 2/ J.J.Degnan, Satellite laser ranging, current status and future prospects, IEEE, Geoscience nad remote sensing, Vol.GE-23, No.4
- 3/ I.Prochazka, Picosecond laser ranging using photodiode in this proceedings

MICROCHANNEL/DYNODE
PHOTOMULTIPLIERS
COMPARISON EXPERIMENT

I. Prochazka, K. Hanal
Czech Technical University
Faculty of Nuclear Science and Physical Engineering
Brehova 7, 115 19 Prague, Czechoslovakia

J. Gaignebet
C.E.R.G.A, Grasse
France

Goals

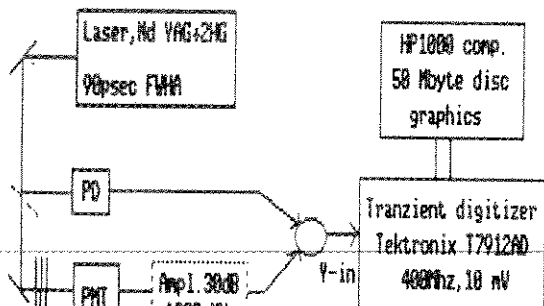
- measurements :
 - * jitter at single/multi PE signal level
 - * time walk (int. delay/amplitude) dependence
 - * ultimate jitter limits
- comparison :
 - * microchannel plate PMT Varian
 - * dynode type PMT RCA8852 (3mm spot)

I. Prochazka, K. Hanal, J. Gaignebet
Microchannel/Dynode Photomultiplier Comparison Exper. 0

I. Prochazka, K. Hanal
Microchannel/Dynode Photomultiplier Comparison Exper. 1

PMT test experiment

PMT test chain characteristics



- Laser - Nd YAG + 2HG, 90 psec FWHM
- Tranzient - 400MHz, 10 nV / div
- 17912AD - sweep speed 20 psec/pixel (MCP)
40 psec/pixel (dynode)
- amplitude resolution 512 levels
- jitter - Pd (vacuum) + Tranzient 23 psec

Fig. 1

Tranzient record processing :

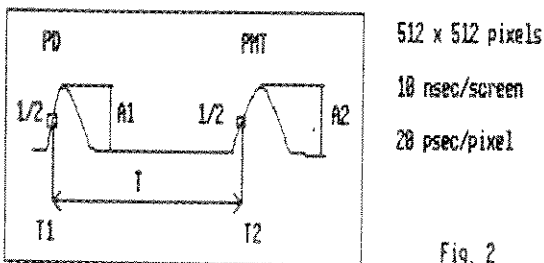


Fig. 2

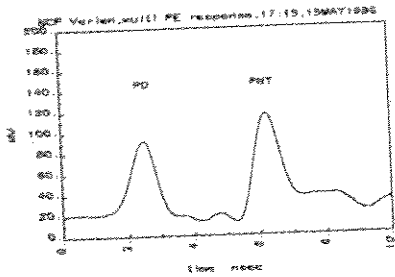
Limitation - dynamic range 5 : 1

I. Prochazka, K. Hanal, J. Gaignebet
Microchannel/Dynode Photomultiplier Comparison Exper. 2

I. Prochazka, K. Hanal, J. Gaignebet
Microchannel/Dynode Photomultiplier Comparison Exper. 3

Microchannel plate PNT, Varian

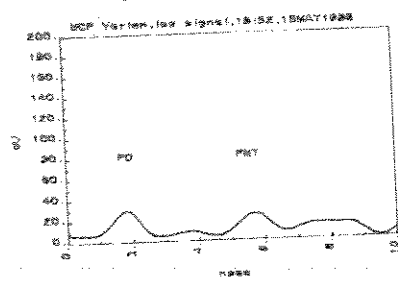
Multi PE signal response



jitter 65 psec

Fig. 3

Low signal response

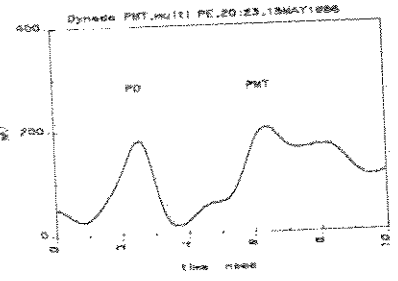


jitter 185 psec

Fig. 4

Dynode PNT, RCA 8852, 3 mm spot on photocathode

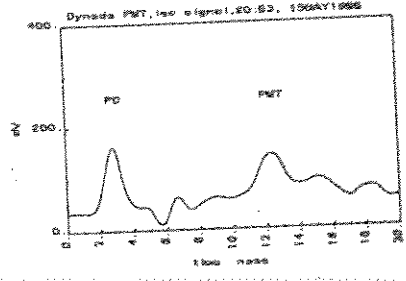
Multi PE signal response



jitter 95 psec

Fig. 5

Low signal response



jitter 290 psec

Fig. 6

I. Prochazka, K. Hanal, J. Gaignebet
Microchannel/Dynode Photomultiplier Comparison Exper.

4

I. Prochazka, K. Hanal, J. Gaignebet
Microchannel/Dynode Photomultiplier Comparison Exper.

5

PNT internal delay versus amplitude

Low signal

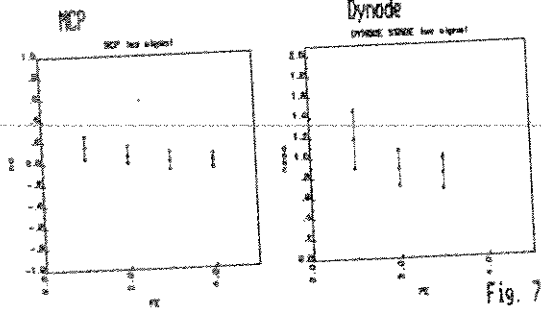


Fig. 7

Strong signal

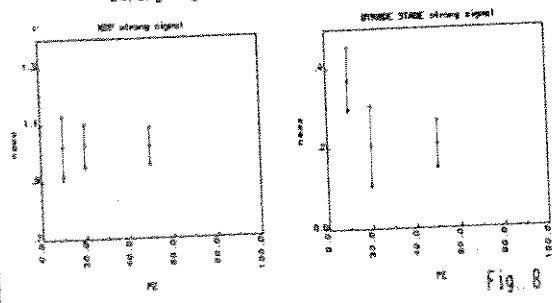


Fig. 8

I. Prochazka, K. Hanal, J. Gaignebet
Microchannel/Dynode Photomultiplier Comparison Exper.

6

PNT jitter comparison summary

	PMT type	PNT type	
		MCP	Dynode
		Varian	RCA8852
Jitter	1 PE	185 psec	290 psec
	10 PE	100 psec	150 psec
	100 PE	65 psec	95 psec

I. Prochazka, K. Hanal, J. Gaignebet
Microchannel/Dynode Photomultiplier Comparison Exper.

7

DETECTORS FOR III.GENERATION LASER RANGING SYSTEMS

Z. Neumann
Astronomical Institute
Czechoslovakia Academy of Sciences

Telephone (0204) 999201

ABSTRACT

Possible detectors are described and their properties jitter, gain, spectral response and noise are considered. The avalanche photodiodes are described in some detail.

The accuracy of transit time depends on - laser pulse width, accuracy of time counter, time property of photodetecting element, frequency properties of cables, type of discriminator, time properties of electronic circuits.

It is possible to generate a pulse width below 100 ps by mode-locking, it influences the detection accuracy (at one photoelectron level) by 40 ps approximately (see lit./1/, relation 2.14). In case of one photoelectron detection level, the accuracy almost does not depend on the type of the discriminator used (see lit./3/ table 1). The top time counters reach the accuracy level better than 40 ps (HP 5370). There are cables for frequencies over 10 GHz and with a convenient arrangement (discriminator as near as possible to the detector) the influence of cables is below 10 ps. It is possible make electronic circuits with jitter below 20 ps. Thus, the transformation of light pulse into the electric one by a photodetector is the main effect that determinates the transit time accuracy.

The case of a photodetector for a start impulse is relatively simple. It is possible to use an intensive light pulse so that no amplification is necessary. The absorption process is fast enough and it implies that the time properties depend on passive elements (encasing, parasitic capacity, inductance etc.). It is possible realize photodetectors, see lit./10/,/11/, such as having a jitter below 10 ps. For the start impulse we can use photoresistor, PIN photodiode, Schottky photodiode etc.

The case of a photodetector for the stop impulse is more difficult. One photoelectron or some photoelectron detection level implies the need of a high subsequent amplification ($10^6 - 10^7$). Up today solution by the usage of photomultipliers is limited. The photomultipliers reach a sufficient gain, however, the principle of photomultiplier activity causes the best photomultipliers having the jitter of approximately 500 ps (see lit./3/,/4/). Therefore, the photomultiplier limits the resultant accuracy to a value of appro-

ximately 7 cm.

What are the possibilities of improving? The usage of microchannel plate photomultipliers is one solution. They reach a sufficient gain of 10^7 and maybe also a convenient jitter with regard to their time response of approximately 250 ps (FWHM). The comparison of this value with the time response of best photomultipliers (approximately 5 ns) and with their jitter (see lit./3/,/4/) shows the probable jitter of microchannel photomultipliers being of about 30 ps.

The other possibility is to look for some other devices acting on an other principles. The need to detect a single photon implies the necessity of amplifying in the same device where the photon is detected. So, main attention among semiconductor devices is directed to the avalanche photodiode.

The amplifying effect of avalanche photodiodes is based on the knocking-out the electrons from a valence in to a conduction band by high energetic electrons and holes. Heterogeneous photodiodes, instead of homogeneous ones, are used to decrease the dark current. They consist of absorption and avalanche regions, see fig. 1 . Photon is detected in the

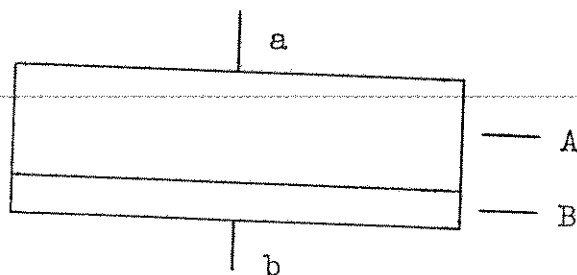


Fig. 1 Schematic illustration of an avalanche photodiode
A - absorption region, B - avalanche region, a - negative outlet, b - positive outlet

absorption region (A). The free electron penetrates into the avalanche region (B) where it induces an avalanche propagation. Arise free electrons get out by the b outlet, the holes penetrate through absorption region to the a outlet.

Avalanche photodiodes from germanium, silicon or A^3B^5 semiconductor (mainly $In_xGa_{1-x}As_yP_{1-y}$) are under consideration from technology point of view.

Avalanche photodiode, as an amplifier, can operate in two modes - linear amplifier mode and photon counting mode. In the first case, it reaches the gain of approximately 10 to 100 which is a very small value for usage in laser ranging system. In the other case, an avalanche photodiode operates either nearly below breakdown voltage or (a short time) over breakdown voltage. In this mode, the gain reaches a value of 10^6 or higher (for silicon see lit./6/,/9/). This is sufficient for a one photoelectron detection level, too.

The type of the semiconductor used implies a spectral response, see fig. 2 . We can see that all materials are able

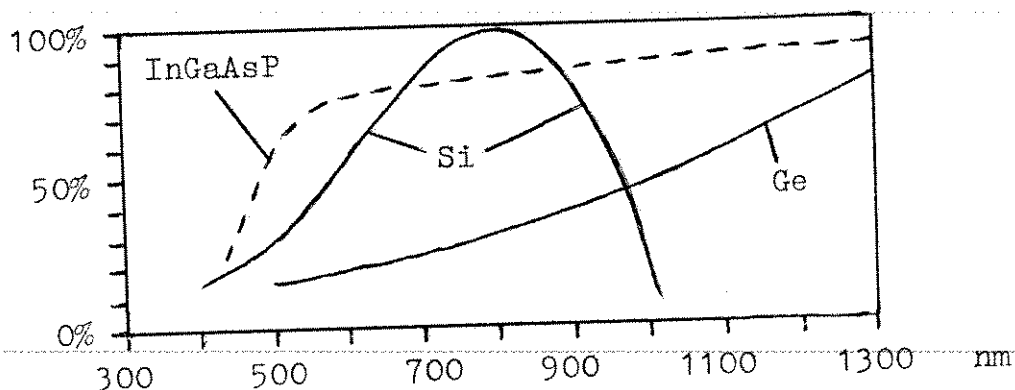


Fig. 2 Spectral response of semiconductor materials
 Comment spectral response of InGaAsP changes according to the relation of components

to detect the radiation with 532 nm wavelength as well as with 1064 nm wavelength.

Total photodiode quantum efficiency at concrete wavelength is determined mainly by the value of absorption coefficient at this wavelength and by the thickness of the absorption layer (and also by antireflection improvement etc.). To obtain a reasonable quantum efficiency (over 10%), a minimal thickness of the absorption layer ought to be of 10 μm

(for 532 nm) and 5 um (for 1064 nm) in case of germanium, of 20 um (for 532 nm) and 100 um (for 1064 nm) in case of silicon and of 1 um (for both wavelength) in case of InGaAsP.

The jitter of an avalanche photodiode is determined mainly by the thickness of the absorption layer. A photon is absorbed randomly on any place of the absorption layer. Due to the different speed of light (approximately 10^8 m.s^{-1}) and electron (approximately 10^5 m.s^{-1}), the delay between a photon coming into the photodiode and the electrical pulse leaving out the photodiode changes according to the place of photon absorption. The jitter implying from this effect reaches approximately 50 ps (10 um layer) and 25 ps (5 um layer) for germanium, 100 ps (20 um layer) and 500 ps (100 um layer) for silicon and 5 ps (1 um layer) for InGaAsP.

The signal-to-noise ratio is not constant (depending on gain) at avalanche photodiodes, as it is in the case of photomultipliers, but it decreases as the gain increases. This dependence is shown on the equation /1/ (according lit./7/)

$$s:n = \frac{K_1 \cdot P^2 \cdot M^2}{(K_2 \cdot P + 2 \cdot e \cdot I_d) \cdot M^2 \cdot F \cdot K_3 + K_4}, \quad /1/$$

where K_1 to K_4 are constants, M is the gain, P is the optical power, I_d is the dark current, e is the electronic charge and F is the excess noise factor depending on the semiconductor material. If the ionization coefficients of electrons and holes are equal, the noise power increases as M^3 but the signal one only as M^2 . When the ionization coefficients are very different, the noise power increases also as M^2 . The biggest difference between the ionization coefficients reveals silicon. In the case of InGaAsP the difference depends on the ratio between the components.

It is reasonable to describe the noise properties of a

photodetector for laser ranging instruments by the frequency of noise pulses instead by its noise power. According to data from lit./6/ - the dark current 18 nA and a gain of $2 \cdot 10^4$ (at temperature 25°C) - it is possible to compute the frequency of noise pulses of 5 MHz. According to data from lit./9/ - the dark current 10^{-13} A and the gain 250 (at the temperature -22°C) - the frequency is equal to 2500 Hz. It is possible to compute, according to data from lit./8/ - dark current $3 \cdot 10^{-10}$ A and the gain 100 - the frequency of noise pulses 20 MHz for InGaAsP .

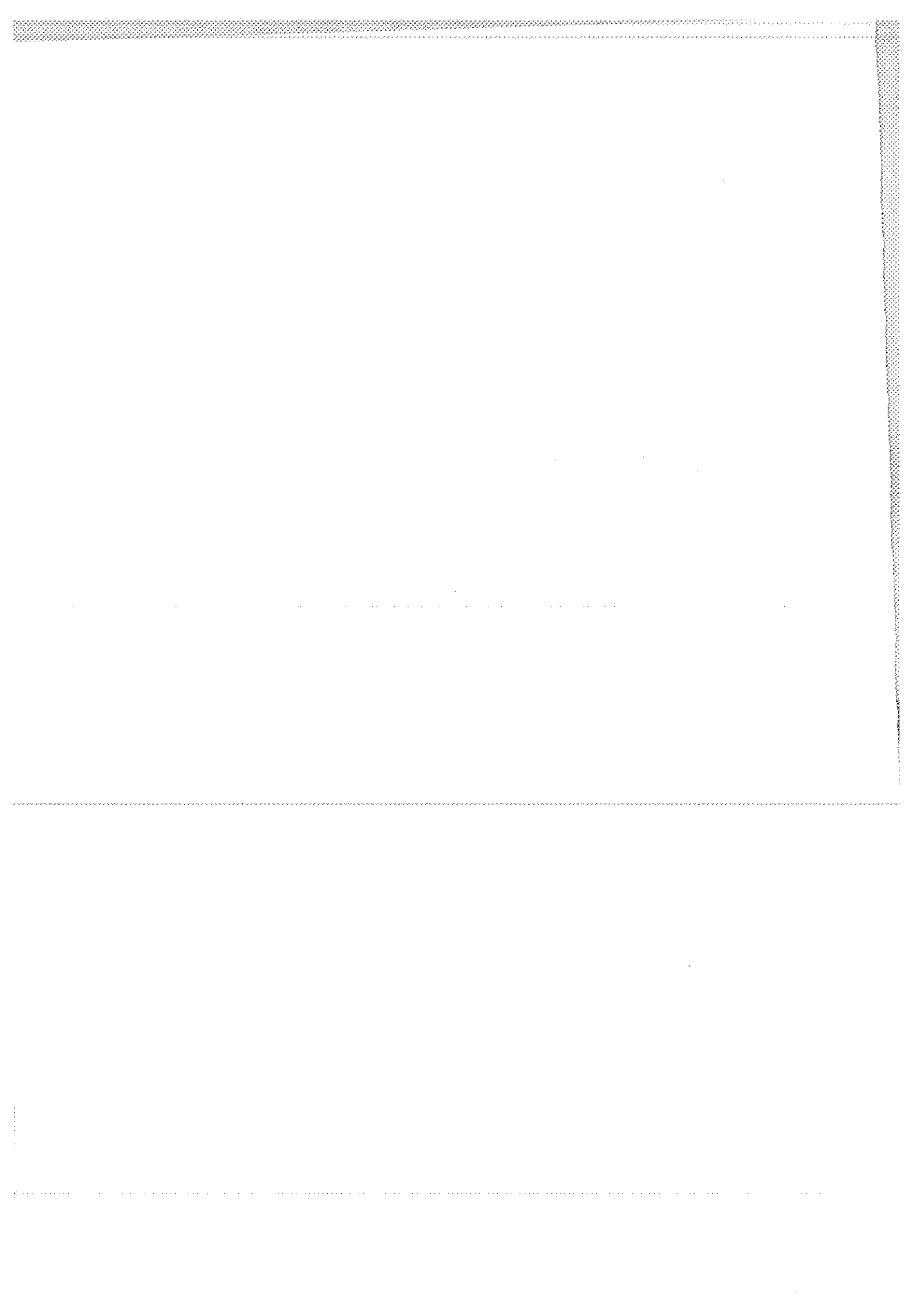
Conclusion : The microchannel photomultipliers and silicon avalanche photodiodes with an approximately 20 μm thick absorption layer (and probably cooled) are convenient for stop impulse detection of 2. harmonic of the Nd:YAG laser for III. generation laser ranging instruments.

Only silicon avalanche photodiodes with approximately 20 μm thick absorption layer (for small jitter) in the photon counting mode seem to be convenient for stop impulse detection of 1064 nm wavelength. The quantum efficiency (due to thin absorption layer and small absorption coefficient) is small, of about 2 to 3%.

For the future, after improving the technology, the InGaAsP avalanche photodiodes seem to be most perspective photodetectors (see lit./7/ pages 413-414). A detection of not only 532 nm, but also of 1064 nm wavelength radiation with high quantum efficiency and a very small jitter will be probably possible in the case of convenient ratio between the components. The jitter will be probably so small to make it reasonable to consider their usage in a two-colour laser instruments (instead of streak camera). Different ionization coefficients enable to reach small noise. The gain 10^6 or more will be probably reached in the photon counting mode.

Literature

- /1/ Matti Paunonen : Studies on the Metsáhovi Satellite Laser Ranging System
- /2/ Centre National D'Études Spatiales, GRGS : Starlette
- /3/ K. Hamal, I. Procházka, J. Gaignebet : Mode Locked Train YAG Laser Calibration Experiment, Observations of Artificial Earth Satellites 23/1984
- /4/ R. Neubert, B. Ritschel, L. Grunwald : Ambiguity and Resolution of a Mode-locked Train Laser Radar, paper on the International Scientific Seminar "Laser Satellite IInd and III^d generation ", 26-30 May 1986, Sofia
- /5/ Specification VPM-221D (2 MCP's) Photo Plate Detector, Varian
- /6/ private information
- /7/ T.P. Pearsall : GaInAsP Alloy Semiconductors, John Wiley and Sons, 1982
- /8/ Kishi, Y and others : Liquid-phase-epitaxial growth of InP/InGaAsP/InGaAs Buried-structure avalanche photodiodes, Electronic Letters, Vol.20,page 165
- /9/ Photonics Spectra, June 1986, page 52
- /10/Roth,W.,SchumacherHH., Beneking H. : Fast Photoconductive GaAs detectors made by laser stimulated MOCVD, Electronic Letters, Vol.19,nom.4, page 142
- /11/Wang S, Y., Bloom D. M. : 100 GHz Bandwidth Planar GaAs Schottky Photodiode, Electronics Letters, Vol.19,nom.14. page 554



THE USE OF GEIGER MODE AVALANCHE PHOTODIODES FOR PRECISE
LASER RANGING AT VERY LOW LIGHT LEVELS :
AN EXPERIMENTAL EVALUATION

S.R. Bowman, Y.H. Shih, C.O. Alley
Department of Physics and Astronomy
University of Maryland
College Park, Maryland 20740 - USA -

Telephone (301) 454 - 3405
Telex 908787

ABSTRACT

Measurements have been conducted to determine the utility of commercially available silicon avalanche photodiodes as detectors in single photon ranging systems. When cooled and operated in a gated Geiger mode these detectors offer an attractive alternative to photomultipliers.

Seven different types of diodes were evaluated for Geiger mode operation. Characteristics such as dark noise and temporal response were used to select the best diode types. Response time studies were conducted on the selected diodes at very low light levels using a mode-locked frequency doubled Nd-YAG laser and a picosecond resolution streak camera system. Single photon response time distributions with standard deviations as small as 90 picoseconds were observed.

Detection efficiency at the singles level was also studied. Using a parametric down conversion process to generate a source of correlated photon pairs, the absolute single photon detection efficiency was measured at 532 nanometers. Efficiencies of 28 % were observed and changes in the detection efficiency with gating voltage were studied.

Results from low and moderate intensity laser ranging with Geiger mode diodes are discussed. The ranging results acquired at the Goddard Optical Test Facility include both terrestrial targets and the Laser Geodynamics Satellite, LAGEOS.

measurements. In this application "echo" pulses are not a significant problem.

Qualitatively the theory of Geiger mode operation is quite simple. The combination of low temperature and a high reversed biasing potential produces an essentially carrier-free region in the junction and depleted intrinsic region of a P+N diode, Figure 1. When a carrier is produced in the depleted region it will move into the high field region of the junction and undergo avalanche amplification as large as 10^9 . The resulting current pulse will continue until voltage across the diode falls to below the breakdown voltage.

Geiger mode operation is easy to observe. The circuit in Figure 2 is cooled to -60°C using dry ice. Reverse bias is applied through a current limiting resistor to bring the diode to within a few volts of breakdown. An additional gating voltage pulse is capacitively coupled onto the diode. In this way the diode can be overvoltaged by as much as several hundred volts during the time of an expected signal. (If the diode is kept in almost total darkness the full voltage can be applied continuously. Most of the silicon diodes tried exhibited dark count rates of less than 100 Hertz at this temperature.) When the diode does break down the resulting pulse is large, usually several volts. This is a great advantage when working with lasers or other electrically noisy devices.

DETECTION EFFICIENCY

To determine their usefulness as laser ranging detectors, several different avalanche photodiodes were purchased. They were selected for large active area, high responsivity, and low cost. Each was tested for Geiger mode operation. Diodes that either failed to exhibit Geiger mode or had dark count rates above one kilohertz were rejected. Figure 3 illustrates relative measurements made to determine the optimum diode operating conditions. Measurements were made to determine detection efficiency and temporal response.

Accurate measurements of the detection efficiency of silicon Geiger diodes were made using a technique first described by D.N. Klyshko.⁵ Conceptually, this is a very simple technique. A single weak laser beam passes through a nonlinear crystal that is phase matched for non-collinear parametric frequency halving. With proper spectral filtering, the result will be two very weak beams having the same wavelength. In fact, energy conservation requires that an equal number of photons, N , are simultaneously created in each beam. Two very sensitive detectors are used to count photons in each beam. The number of counts in each beam, N_1 and N_2 , are recorded. Also, the number of coincidence counts, N_c , is recorded. The absolute detection efficiencies, η_1 and η_2 can then be calculated from the simple relations:

$$N_1 = \eta_1 N \quad N_2 = \eta_2 N \quad N_c = \eta_1 \eta_2 N.$$

Figure 4 details the actual device set up to realize the Klyshko technique at the wavelength of interest, 532 nanometers. The results of measurements using two RCA C30902E diodes were maximum single photon detection efficiencies of 21

$\pm 3\%$ and $28 \pm 3\%$.

TEMPORAL RESPONSE

In addition to detection efficiency, the temporal response of the diodes was studied. Three important properties of the Geiger pulse were measured. They were amplitude stability, pulse risetime, and internal delay time jitter.

Amplitude fluctuations are a potential source of timing error in any ranging system.⁶ Fortunately, the amplitude of the Geiger pulse is very stable. Under normal conditions "good" diodes have only a few percent variation in pulse amplitude, Figure 5. If the diode is operated at high count rates (greater than 5 kilohertz for d.c. biasing), it will not recharge completely before each firing. The result is a wide spectrum of pulse heights. Some diodes, particularly the RCA C30954E, exhibited frequent echo pulses within 10^{-4} seconds of the leading pulse. The amplitudes of the echo pulses varied substantially again, probably due to lack of charging time.

Rise time measurements on the Geiger diode pulses are summarized in Table 1. All were measured with a load impedance of 50 ohms. A weak dependence of the risetime on temperature and voltage was observed. Lowering the temperature or raising the voltage could shorten the risetime by as much as a factor of two. The fastest rise attained was 1.0 nanosecond. This may be limited by the impedance of the diode packaging, a TO-18 can and socket.

Internal delay jitter was measured in two different ways. The first was to trigger a Hamamatsu C1000 Streak Camera System with the output of a Geiger diode. This system incorporates a C1583 streak camera with a streak trigger jitter of 5 picosecond as measured by the company. After a thousand laser firings, the width of the distribution of camera streaks was measured. Comparing this with the distribution produced by triggering from an ultrafast PIN diode, the internal jitter in the Geiger diode can be found. For the single photon intensity level, the standard deviation of the distribution was 90 picoseconds. These distributions clearly show an increase in the 10% full width trigger jitter from 190 to 360 picoseconds when the moderate intensity was reduced by 10^7 to the single quanta level. This increase in the internal delay jitter at low light levels can be explained in terms of the carrier transit time of the depleted region. At very low intensities the carriers which start the avalanche in the junction are formed throughout the depleted region. The structure of the RCA C30902E diode on which these measurement were made is such that the depletion region and junction are 15 and 2 microns thick, respectively.⁷

Similar results were obtained when the detector was used for terrestrial ranging. Figures 6 and 7 show histograms of the timing spread for ranges to a terrestrial corner cube reflector. With only a factor of 10 difference in the intensities used, the broadening of the distribution is clear. In addition to a 39% increase in the standard deviation, the mean value shifted later by 200 picoseconds. These measurement have 40 picosecond uncertainty associated with the timing electronics used.

Although Geiger mode photodiodes offer many advantages to photomultipliers in the measurement of weak light pulse epochs, they do have a serious drawback. After the avalanche pulse occurs, the diodes experience a relatively long deadtime associated with the carrier lifetimes in silicon. The minimal recovery time was not studied here but is thought to be of the order of 10^{-7} seconds. In this research the recovery time was limited by the RC time constant of the biasing circuit, 10^{-4} seconds. As a result the GM diodes used here were basically single stop detectors. This leads to significant noise blanking when the diodes are used in the presence of high background lighting, photon flux rates above 10^5 Hz. To resolve this problem work is currently under way on a multiple diode detecting package.

RANGING RESULTS

As a final test of utility of the GM photodiodes, laser ranging sessions were conducted using a single RCA C30902E diode as detector. The ranging test were conducted at the 1.2 meter precision tracking telescope on the Goddard Optical Test Site in Greenbelt Maryland. Strong return rates were achieved from the Laser Geodynamics Satellite (LAGEOS) using only two millijoules of transmitted laser energy. The LAGEOS satellite is in a nearly circular orbit with an altitude 6000 kilometers. For ranging at the single photon level, a chi squared fit to a second order polynomial using a typical two minute sample of the resulting timing residuals gave a standard deviation of 192 picoseconds. Figure 8 shows ranging residuals from a typical LAGEOS ranging session where higher laser energies are used to get a nearly one to one signal rate.

Lunar ranging data has also been acquired using the GM photodiode receiver. The results shown in Figure 9 were obtained in five minutes using 100 millijoule pulses under marginal atmospheric conditions. JPL analysis of this data gave a standard deviation of 168 picoseconds or a range uncertainty of 2.8 centimeters.

CONCLUSION

Measurements were conducted with silicon avalanche photodiodes used in a cooled Geiger mode to determine their usefulness in satellite laser ranging systems. Single photon detection efficiencies were measured to be 28% for 532 nanometers. Timing jitters of the single photon responses were found to have a standard deviation of 90 picoseconds. The high quality lunar and satellite ranging results obtained here prove the commercially available GM photodiodes to be an excellent alternative to photomultipliers both in terms of cost and performance.

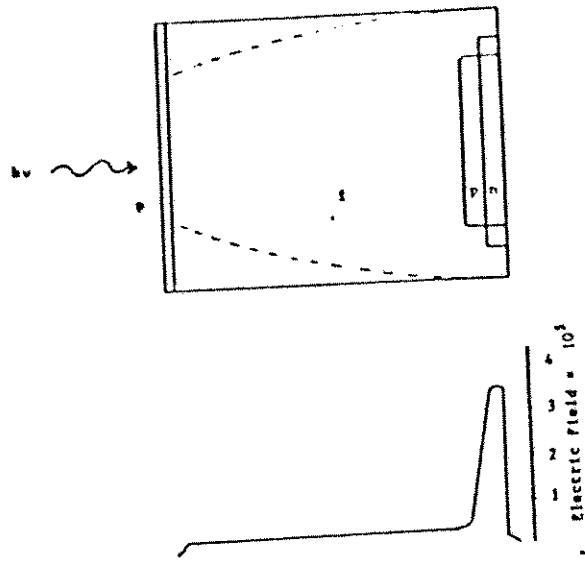
ACKNOWLEDGMENT

The authors would like to thank Bob Hyde for his initial suggestion of this research topic. Thanks also go to John Rayner, Jack Bufton, and Liming Ding for their assistance during this work.

TABLE 1
TYPICAL GEIGER MODE PROPERTIES OF APD'S TESTED
T = -60°C

RCA C309021S	$V_{Brk} = 165 \text{ V}$, $T_{Rise} = 3 \text{ ns}$ Dark count = 16 Hz @ $V_{Brk} + 20 \text{ V}$
RCA C30902E	$V_{Brk} = 170 \text{ V}$, $T_{Rise} = 1.2 \text{ ns}$ Dark count = 100 Hz @ $V_{Brk} + 40 \text{ V}$
RCA C30948E	$V_{Brk} = 192 \text{ V}$, $T_{Rise} = 1.7 \text{ ns}$ Dark count = 50 Hz
RCA C30954E	$V_{Brk} = 140 \text{ V}$, $T_{Rise} = 3 \text{ ns}$ Dark count = 70 Hz @ $V_{Brk} + 20 \text{ V}$
RCA C30955E	No Geiger mode
NDL 1202	$V_{Brk} = 135 \text{ V}$, $T_{Rise} = 1 \text{ ns}$ Dark Count = 2 kHz @ $V_{Brk} + 15 \text{ V}$
NDL 5100 (Germanium)	$V_{Brk} = 30 \text{ V}$, $T_{Rise} = 5 \text{ ns}$ very noisy, triggered immediately, amplitude only 10mV

REACH-THROUGH APD STRUCTURE



From P.P. Webb et al. "Properties of Avalanche Photodiodes,"
R.C.A. Review 35, (1974), 251.

FIGURE 1

GEIGER MODE PHOTODIODE BIASING CIRCUIT

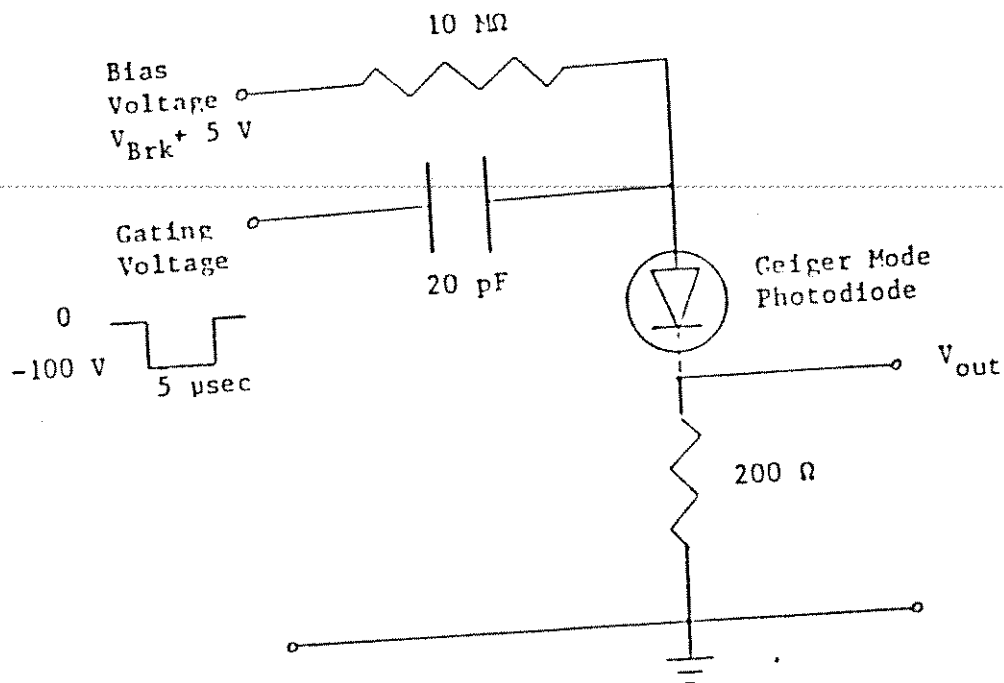


FIGURE 2

GEIGER MODE PHOTODIODE PERFORMANCE VS. VOLTAGE

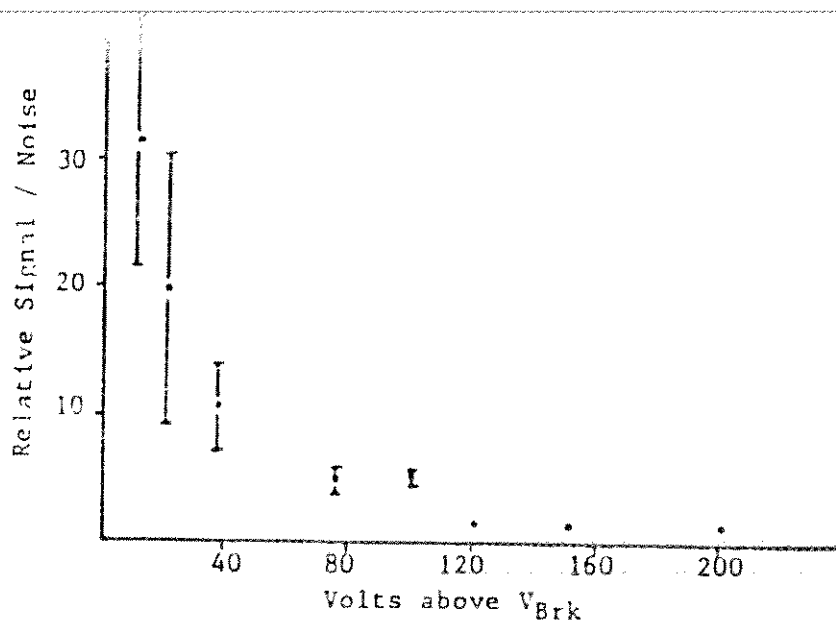
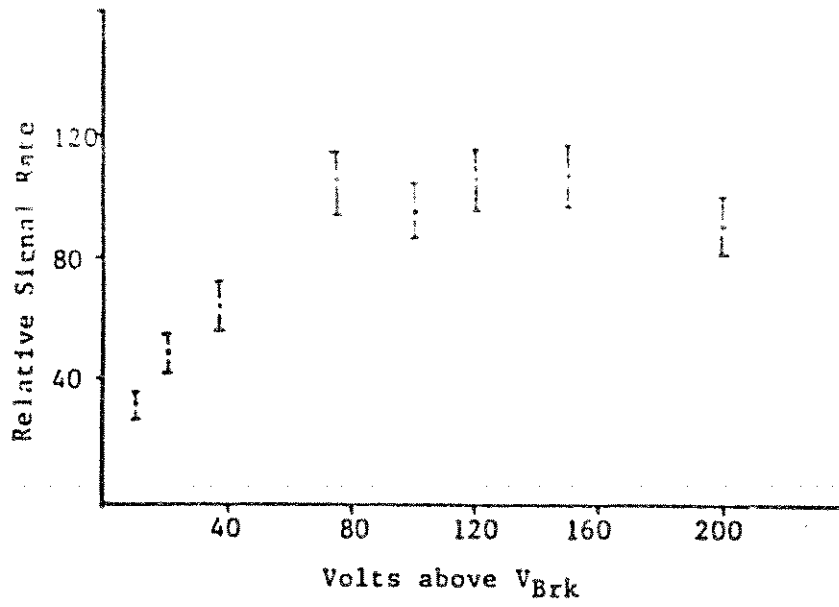


FIGURE 3

KLISHKO DETECTION EFFICIENCY MEASUREMENT

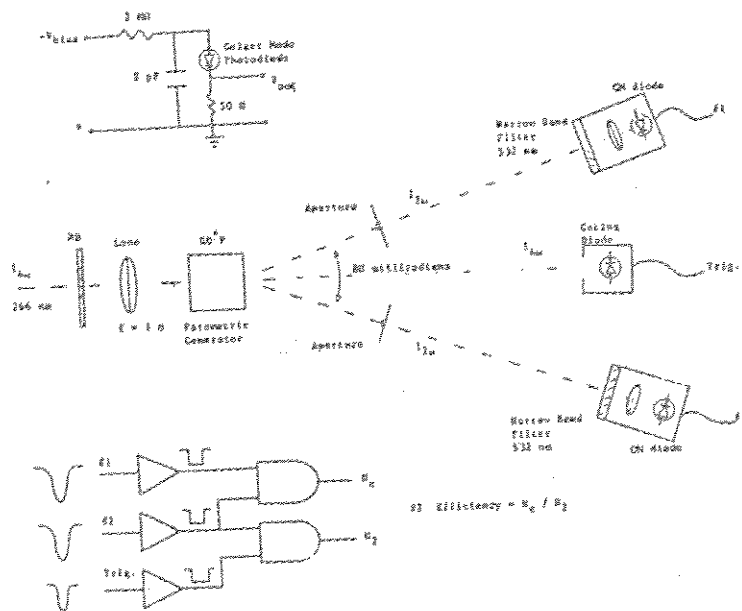
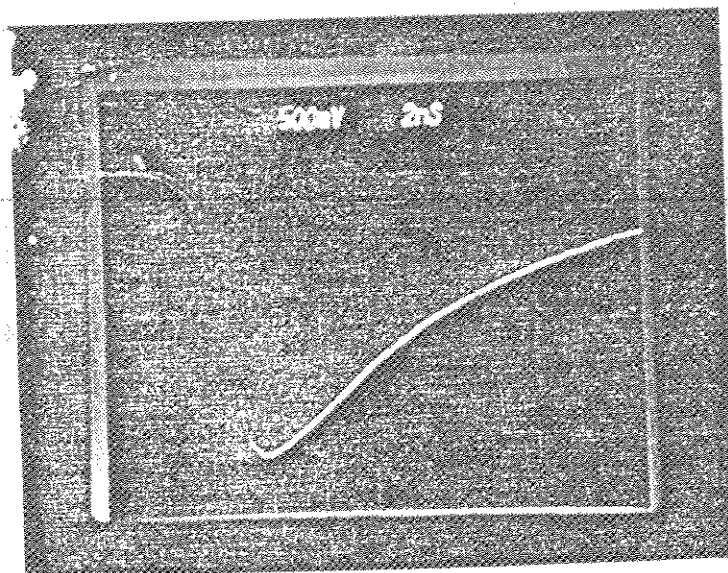


FIGURE 4



RCA30902E DIODE SN 40889, $V_{gate} = -50$ V, $V_{bias} = -160$ V
 Three Pulses, Risetime = 1.2 ns (10490%)
 measured with Tektronics 7104 Oscilloscope

FIGURE 5

TERRESTRIAL RANGING WITH GM PHOTODIODE, ND = 9

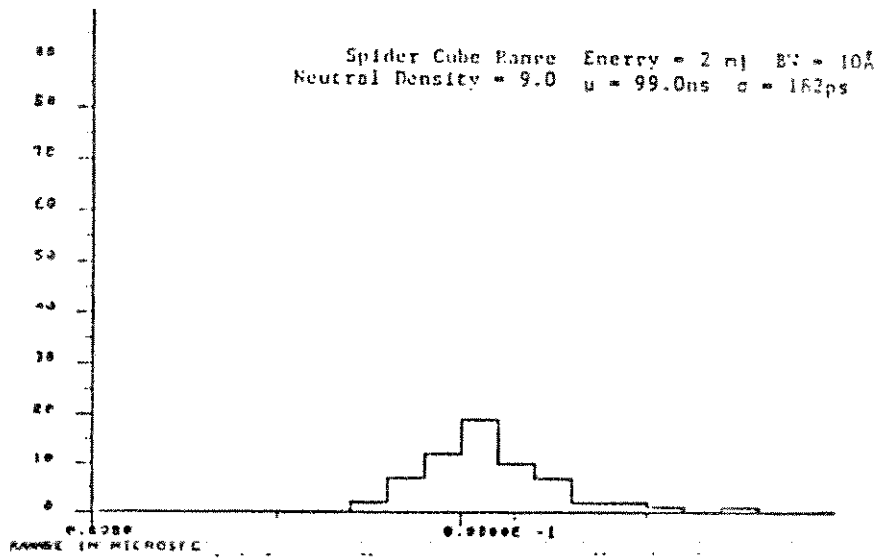


FIGURE 6

TERRESTRIAL RANGING WITH GM PHOTODIODE, ND = 10

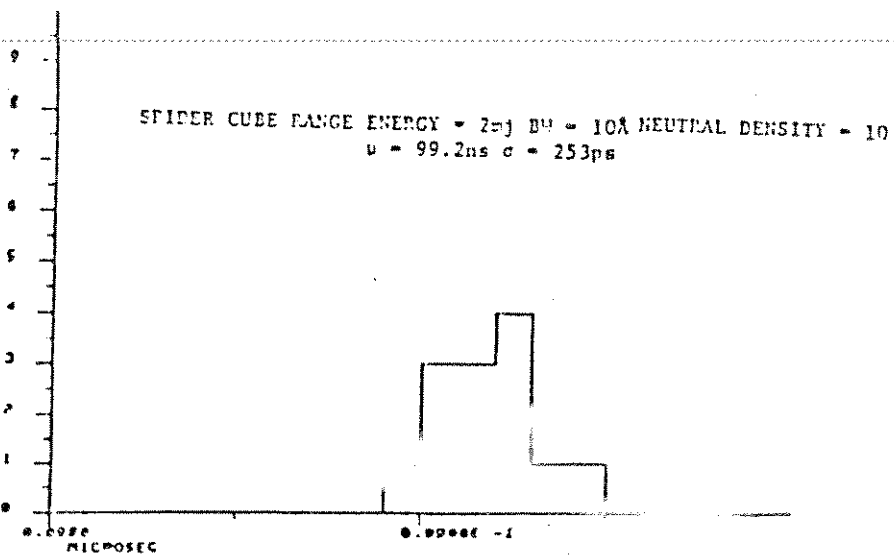


FIGURE 7

SATELLITE RANGING RETURNS

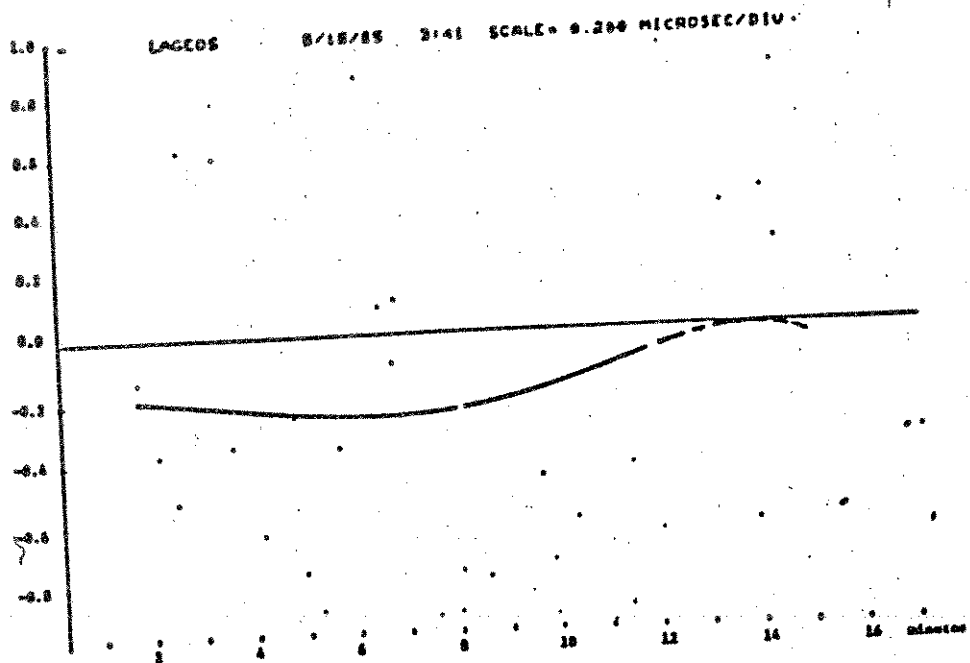


FIGURE 8

LUNAR RANGING RETURNS

HADLEY 8:43 8/26/86

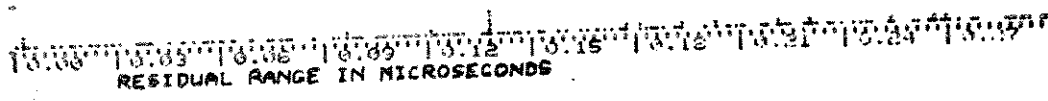
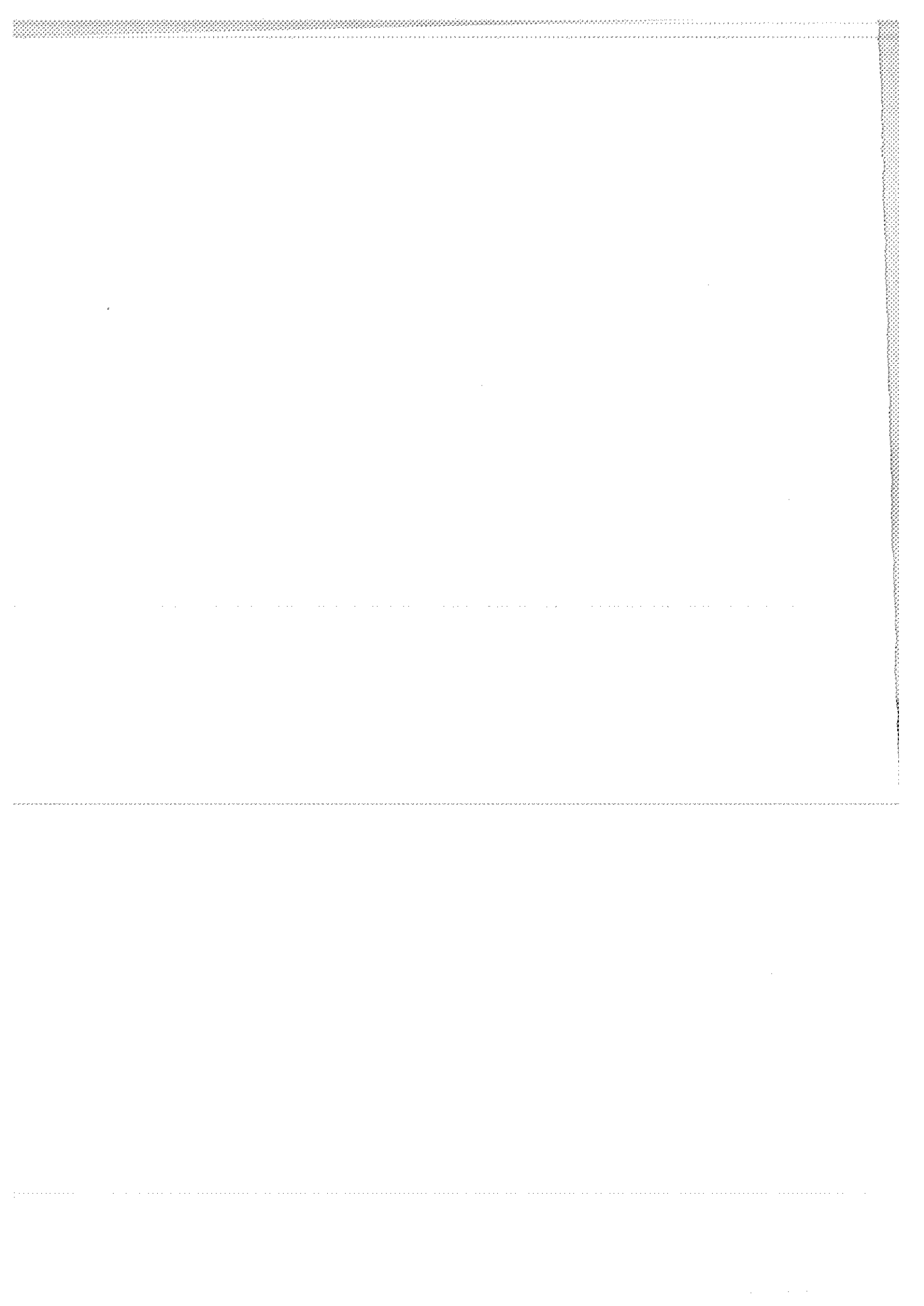


FIGURE 9

REFERENCES

1. R.J. McIntyre, "The Distribution in Gains in Uniformly Multiplying Avalanche Photodiodes : Theory," IEEE Transactions on Electron Devices, ED-19 (1972), 703.
2. T.E. Ingerson, et al., "Photon counting with photodiodes," Applied Optics, 22 (1983), 2013.
3. P.A. Ekstrom, "Triggered avalanche detection of optical photons," J. Appl. Phys., 52 (1981), 6974.
4. P.P. Webb and R.J. McIntyre, "Recent developments in silicon avalanche photodiodes," RCA Engineer, 27-3 (1982), 96.
5. D.N. Klyshko, "Use of Two Photon Light for Absolute Calibration of Photoelectric Detectors," Sov. J. Quantum Electron. 10 (1980), 1112.
6. T.M. Zagwodzki, Test Techniques for Determining Laser Ranging System Performance, NASA Technical Memorandum TM82061 (Goddard Space Flight Center, Greenbelt, MD. Jan. 1981).
7. Webb and McIntyre, p.100.



SINGLE PHOTON SOLID STATE DETECTOR
FOR RANGING AT ROOM TEMPERATURE

K. Hamal, H. Jelinkova, I. Prochazka, B. Sopko
Czech Technical University
Faculty of Nuclear Science and Physical Eng.
Brehova 7, 115 19 Prague, Czechoslovakia

Telephone 848 840
Telex 121254 FJFI C

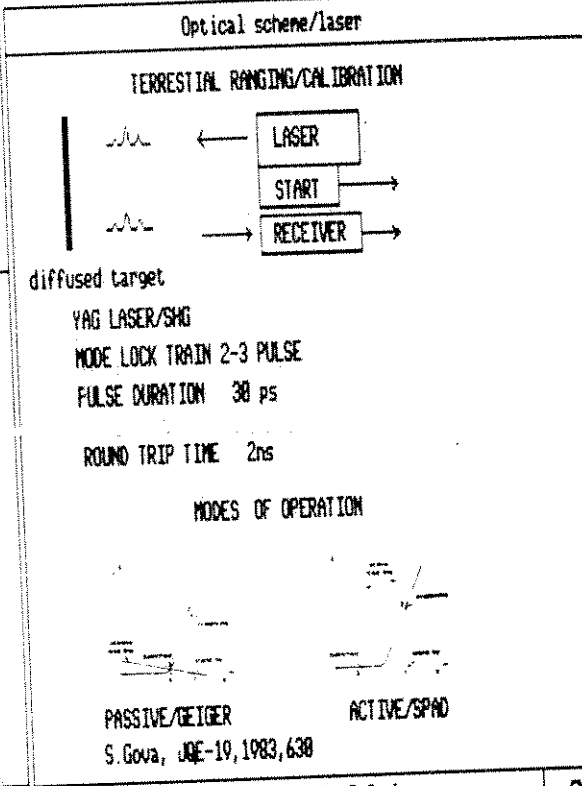
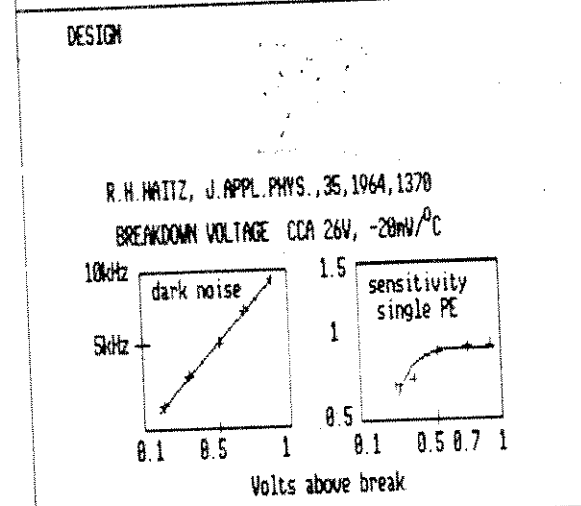
ABSTRACT

To detect return signal at satellite/lunar laser ranging stations, mostly photomultipliers are exploited. There is a strong interest to exploit solid state detector. We developed a solid state detector operating at single and multiphoton level at room temperature. The quantum efficiency is 10/2% at 0.53/1.06 μm . The timing jitter at single photon detection is 100/220 psec at 0.53/1.06 μm . Two modes of operation: active and passive quenching have been exploited.

Photodiode for ranging

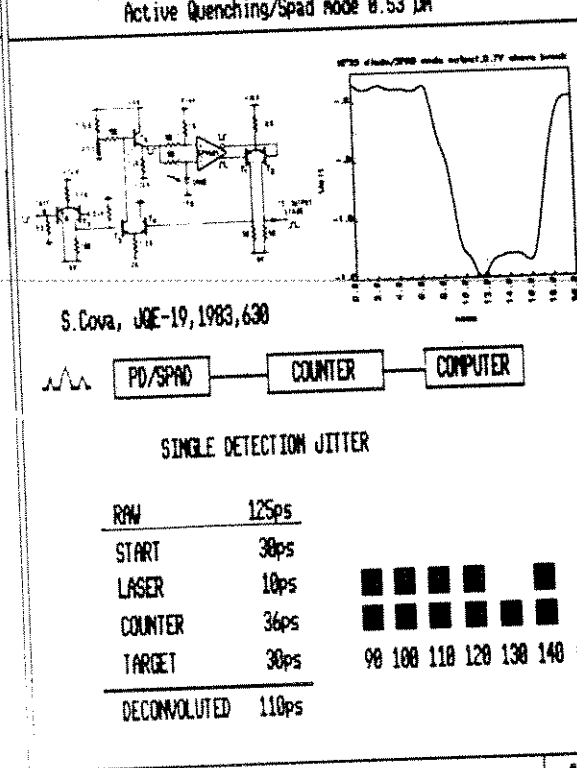
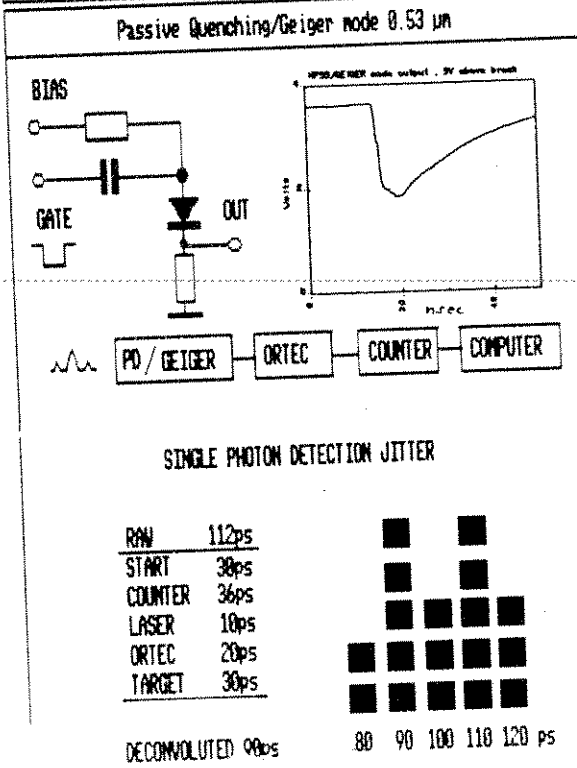
RANGING DETECTOR - REQUIREMENTS

JITTER	LOW
QUANTUM EFFICIENCY	HIGH
WAVELENGTH	0.4 - 1.08 μm



K. Hanač, H. Jelinková, I. Procházka, B. Šopko
Single Photon Solid State Detector For Ranging ... 1

K. Hanač, H. Jelinková, I. Procházka, B. Šopko
Single Photon Solid State Detector For Ranging ... 2

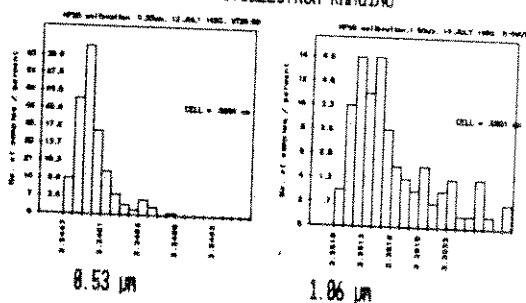


K. Hanač, H. Jelinková, I. Procházka, B. Šopko
Single Photon Solid State Detector For Ranging ... 3

K. Hanač, H. Jelinková, I. Procházka, B. Šopko
Single Photon Solid State Detector For Ranging ... 4

Active Quenching / 0.66 μm

SINGLE PHOTOELECTRON RANGING



1.06 PHOTON PENETRATES NEUTRAL REGION

RAW	225ps
START	30ps
LASER	18ps
ORTEC	20ps
COUNTER	36ps
TARGET	30ps

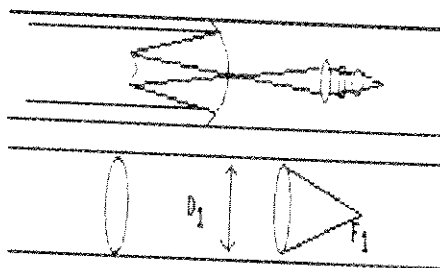
DECONVOLUTED 220ps

K. Hanal, H. Jelinkova, I. Prochazka, B. Sopko
Single Photon Solid State Detector For Ranging ...

5

Field of View / Max. Beam Divergence

RECEIVER OPTICS



TRANSMISSION EFFICIENCY

$$\eta = \frac{\eta_{\text{diode}} (f_1/D_1)^2}{\theta_R^2 \cdot D^2}$$

IF $\theta = 45^\circ$, $f_1/D_1 = 1$, $\eta = 1$

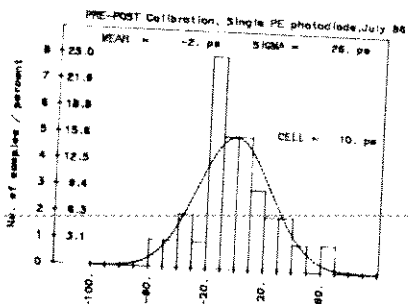
$$\theta_R \text{ LIMIT} = \frac{45 \cdot 10^{-3}}{D}$$

TELESCOPE DIAMETER	1.5M	1M	0.6M	0.3M
MAX. FIELD OF VIEW	6"	9"	15"	30"

K. Hanal, H. Jelinkova, I. Prochazka, B. Sopko
Single Photon Solid State Detector For Ranging ...

6

System Stability



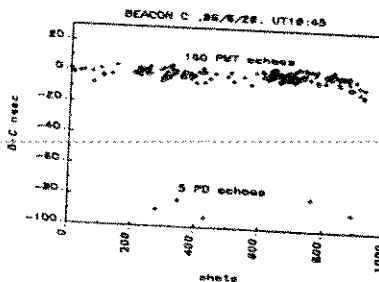
PERIOD JULY 1986
SERIES 100-200 ECHOES
WAVELENGTH 0.53 μm
SINGLE PHOTOELECTRON

K. Hanal, H. Jelinkova, I. Prochazka, B. Sopko
Single Photon Solid State Detector For Ranging

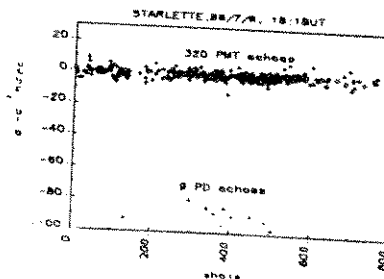
7

Satellite Ranging

BEACON-C



STARLETTE



K. Hanal, H. Jelinkova, I. Prochazka, B. Sopko
Single Photon Solid State Detector For Ranging

8

HPSS diode ruggedness

Diode used as a SLR experimental receiver detector, the system was aligned using corner cube at 100m, accidentally, the MD were missing lasing with the full power

total energy 70 mJ
power flux density 7.000 GW/cm²



NO DAMAGE

K. Hanal, H. Jelinkova, I. Prochazka, B. Sopko
Single Photon Solid State Detector For Ranging ...

Summary / Single Photon Detectors Review

	Hanal et al		PMT dyn./MCP	Bowman et al
	Geig.	SPAD		
JITTER psec	0.53 1.06	98 220	110 220	200 105 253/162/98
QUANTUM EFFICIENCY %	0.53 1.06	10 2	10 2	10-30 0.3 28
DARK COUNT kHz		6	6	< 0.1
DEAD TIME incl. discrimin			150ns	60ns 100 μs
OUTPUT PULSE per Photoel.	2 V	N/A		2-50mV 3 V
RUGGEDNESS		excellent		low/very low excellent
FIELD OF VIEW		9''/1m		no limit
TEMPERATURE		room		room -60° C
DISCRIMINATOR		yes	no	yes yes
POWER SUPPLY		30V		2.5kV/5kV 160 V
GATE		TTL	N/A	HV/HV 50 V

K. Hanal, I. Prochazka, H. Jelinkova, B. Sopko
Single Photon Solid State Detector for Ranging at Room.

"CONSTANT FRACTION" DISCRIMINATORS IN FEW
AND MULTIPHOTOELECTRON LASER RANGING

W.A. Kielek
Departement of Electronics
Institute of Radioelectronics
Warsaw University of Technology
Nowowiejska str. 15/19 00-665 Warsaw - Poland -

Telephone 21007653 or 253929
Telex 813 307

ABSTRACT

The report explains some not widely known properties of c.f. discriminators used in nuclear techniques when using in laser ranging, as for instance mean value of timing point walk with signal energy, and the possibility of jumps in results in some conditions. Accuracy optimization methods are given for the case of the absence of jumps.

"CONSTANT FRACTION" DISCRIMINATORS IN FEW- AND MULTIPHOTOELECTRON LASER RANGING

W.A. Kielek
Department of Electronics
Institute of Radioelectronics
Warsaw University of Technology
Nowowiejska str. 15/19 00-665 WARSAW, POLAND

Telephone 21007653 or 253929
Telex 813 307

ABSTRACT

The report explains some not widely known properties of c.f. discriminators used in nuclear techniques when using in laser ranging, as for instance mean value of timing point walk with signal energy, and the possibility of jumps in results in some conditions. Accuracy optimization methods are given for the case of the absence of jumps.

1. GENERALITIES

Almost all so called "constant fraction" discriminators use the principle of work as follows [1], [2], [3], [4]: from the input signal attenuated in accordance with fraction value, the input signal unattenuated but properly delayed is subtracted, and resulting signal is examined for zero - crossing. After that subtraction, one obtains the signal

$$\psi(t) = f \cdot f(t) - f(t - T_d) \quad (1)$$

where: f - fraction, T_d - delay, $f(t)$ - input signal.

This operation is done using for instance block schemes as at Fig. 1. All ORTEC, TENNELEC 454 and 455, EG&G and almost all other c.f. discriminators used in nuclear technics follow this principle of work. The independence of timing point on the amplitude of incoming pulses is preserved in case of constant deterministic shape of them. This situation is illustrated at the Fig. 2. There is the single zero - crossing only in case of that deterministic pulse signal case.

The signal at the PMT output, it is the sum of random Poisson number of PMT single-photoelectron responses, each of deterministic shape, but of random amplitude. The single realisation of that signal can be described by the formula:

$$f(t) = \sum_{i=1}^K g_i f_{SER}(t - t_i - \tau_i) \quad (2)$$

where: K - Poissonian number of photoelectrons realised, g_i ,

t_i, τ_i - random variables: PMT gain, times of PE generation at the photocathode, and delay in PMT, respectively; $f_{SER}(t)$ - deterministic shape of single PE (photoelectron) response of PMT. Due to existence of the sum $t_i + \tau_i$ in parentheses of formula (2), it is clear that probability density of PMT delay curve has got the same effect on the accuracy as the laser pulse shape, and the "equivalent" laser pulse can be introduced, of the shape of the convolution of laser pulse and PMT delay density curve. In case of single - photoelectron signal the shape of the signal is the same in each realisation. It is also true when the signal is composed of few or many PE but the length of the laser pulse and PMT delay density curve is very short in comparison with the single electron response pulse of the PMT tube.

2. POSSIBILITY OF JUMPS

When it is not the case, the shape of the input signal is random, not the same in each realisation. For few PE in realisation of the signal, and sufficiently small relation between widths of f_{SER} and convolution of the laser pulse and PMT delay density curve, the width of f_{SER} is not enough to make one smooth pulse signal. There is the group of separated f_{SER} pulses with breaks between them. The signal can be also of the form of the multi - top single pulse. In both such cases the resulting signal at the input of the zero - crossing sensitive trigger can have more than one zero - crossing (Fig. 3). The time position of work of the discriminator jumps from the right position to the first zero - crossing. This effect produces the increase in standard deviation and decrease in the mean value of results.

Especially severe influence on the results can have this effect, when the laser signal is not well limited in time, for instance when the main signal pulse stands at some pedestal of weaker radiation (e.g. when using pulse chopper), or when laser pulse is a Gaussian pulse. For such signal, in few - and multi - PE work there exists the possibility to obtain the jumps in results in the direction to decrease the result by few nanoseconds.

This phenomenon is illustrated at the Fig. 4 (Gaussian signal pulse). Single photoelectrons generated by the weak laser radiation before main part of the signal can move in some realizations the time point of work of zero - crossing trigger from the right position to the wrong position few ns before the right one.

At low energies, there is no this effect due to small probability of generation of photoelectrons far before the central part of the laser pulse. At higher energies, when the photoelectron number is high, there exists the high probability of compensation of the influence of the first photoelectrons by the subsequent ones. The probability to obtain false zero - crossing at the summing point in the circuit is again small. The max. probability lies in the medium energy region, between 20 and 1000 PE, dependent on parameters such as fraction, filtration and delay.

It can be deduced from signal model and formula (1) that

probability of jumps should be smaller when: increasing the delay of delay line, or / and the filtration F, or / and the fraction value f. These statements are confirmed by simulations and experiment in laboratory and at the 1-st generation laser stations. Simulation results are given at Figs. 5 and 6.

3. WALK IN THE CASE OF ABSENCE OF THE JUMPS

But also when the jumps are absent, there is no possibility to obtain no delay walk with energy when using c.f. or fixed threshold discriminators. Suppose the symmetrical shape of the "equivalent" laser pulse. In case of the single photoelectron in the signal, the mean position of this photoelectron is in the centre of this pulse, say zero, due to equal probabilities of negative and positive values of PE position. But in case of two photoelectrons, the probability of positive value of position of both photoelectrons is 25% only. Then, the probability of existence of at least 1 PE on the left side from the zero position is 75% (50% for single PE). For very high PE number, the PMT output signal has got the shape of the f_{SER} convolution with the "equivalent" laser pulse shape, and the timing point goes to the negative position in accordance with the fraction value. Then, for the signal following (2), the walk is unavoidable even in the ideal case of no walk for deterministic signal shape. Some results for walk obtained from simulations are given at Fig. 5.

4. STANDARD DEVIATION

There exists the proof, that normalised to the pulse half-width random error, approximately, for large PE number, follows the formula:

$$\sigma_A/T = g_1 \alpha^{1/2} N^{-1/2} \quad (3)$$

where α is the mean square of the normalised to unity PMT gain, N is the mean PE number, T - half of width of the pulse, or σ parameter of Gaussian pulse.

The g_1 coefficient obtained by simulations is given at the Fig. 6. Fortunately, no jumps are present up to 20 PE energy level. Well limited in time (for instance trapezoidal) waveforms without wide pedestal do not produce the jumps. In case of absence of jumps, this discriminator is quite good, especially for the random error.

The theoretical formula I obtained (remarks about method in [5]) for g_1 coeff. dependent on f, F and w (fraction, filtration and normalised delay respectively) when the signal and filter (PMT) response is of the form of Gaussian pulse is as follows:

$$g_1^2 = \left\{ f^2 \exp \left[- \frac{z+1}{2z+1} A^2 \right] + \exp \left[- \frac{z+1}{2z+1} B^2 \right] + \right. \\ \left. - 2f \exp \left[- \frac{z+1}{2z+1} \left\{ \frac{w^2}{2} \left(z + \frac{1}{2} \right) + \left(\frac{\ln \frac{1}{f}}{w} \right)^2 \right\} \right] \right\} \cdot \\ \cdot \frac{z+1}{z \sqrt{2z+1}} \cdot \left\{ B \exp \left[- \frac{B^2}{2} \right] - f A \exp \left[- \frac{A^2}{2} \right] \right\}^{-2} \quad (4)$$

where: $w^2 = \frac{T_d^2}{\sigma^2 + \sigma_F^2}$, T_d - delay time at Fig. 1, $z = (\sigma/\sigma_F)^2$
 $F = (\ln 2)^{1/2} \cdot \sigma_F/\sigma$

$A = \frac{w}{2} - \frac{\ln \frac{1}{f}}{w}$, $B = -\frac{w}{2} - \frac{\ln \frac{1}{f}}{w}$, σ , σ_F - parameters

of Gaussian signal and filter response, respectively. Computations from formula give the results as at the Figs. 7, 8, 9.

The case of f equals 1, there is also the case of Short Circuited Delay Line shaping and zero crossing detection. The results indicate that proper choice of parameters can give the same standard deviation as for max. likelihood estimation [6].

5. CONCLUSIONS

- A. The mean value change is unavoidable when using C.F. timing in case of changing the energy level from 1 to few PE. That change is proportional to the width of the convolution of laser pulse and PMT delay density curve.
- B. Above 10-20 PE energy jumps in results can exist. This effect is absent for laser pulse waveforms well limited in time.
- C. Probability of jumps decreases when increasing the filtration (f_{SER} width), fraction, delay, and charge sensitivity of zero-crossing trigger or comparator.
- D. In the absence of jumps, for proper values of F , T_d , f parameters, Gedcke-Mc Donald type c.f. discriminator is good, especially for standard deviation, and is only slightly poorer in mean value walk than the c.f. discriminator with peak value memorization [5].
- E. Standard deviation reaches the minimum for much higher delay values than the value which is needed to obtain constant fraction work for the deterministic signal.

REFERENCES

1. D.A.Gedcke, W.J. Mc Donald. Nucl. Instr. Methods 55, 1 (1967).
2. M.R.Maier, P.Sperr. Nucl. Instr. Methods 87, 13 (1970).
3. T.J.Paulus, M.O.Bedwell. "High Speed Timing Electronics and Applications of Hybrid Electronics in Nuclear Instrumentation". ORTEC Inc.
4. Instructions and data sheets for ORTEC and other c.f. discriminators.
5. W.Kiełek. V-th Workshop on Laser Ranging Instrumentation, Proceedings, p. 112-118.
6. I.Bar David. IEEE Trans. on Information Theory, IT-15, 31 (1969).

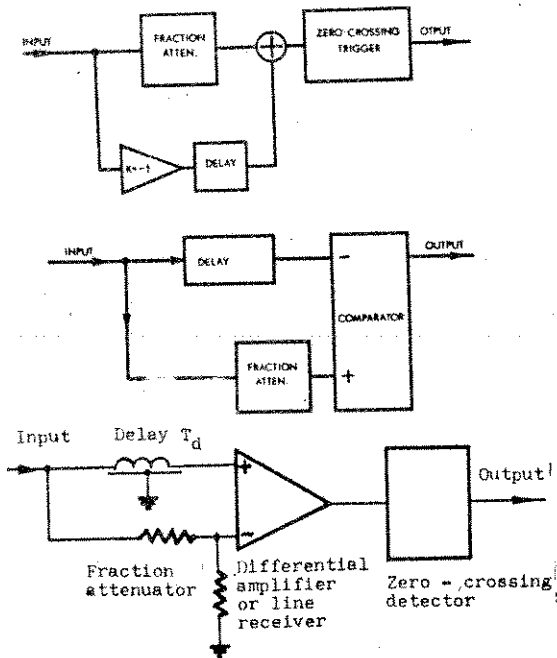


Fig. 1 Variants of principal scheme of nuclear "c.f." discriminators

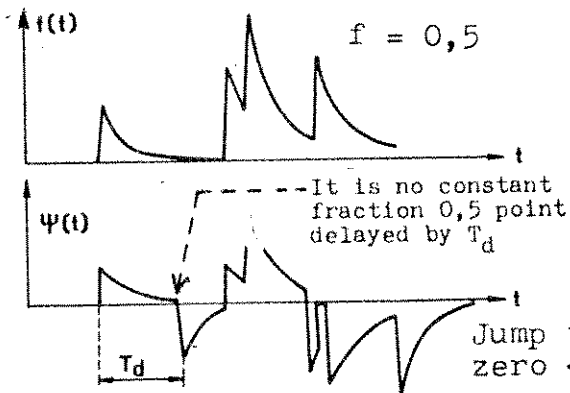


Fig.3 Illustration of work of the circuits from Fig.1, few PE, stochastic signal

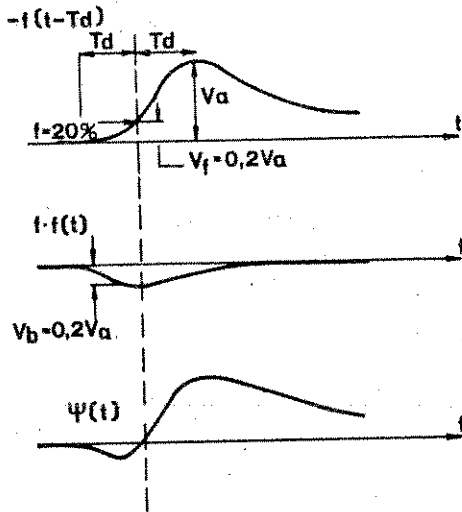


Fig.2 Illustration of work of the circuits from Fig.1, deterministic in shape single signal pulse

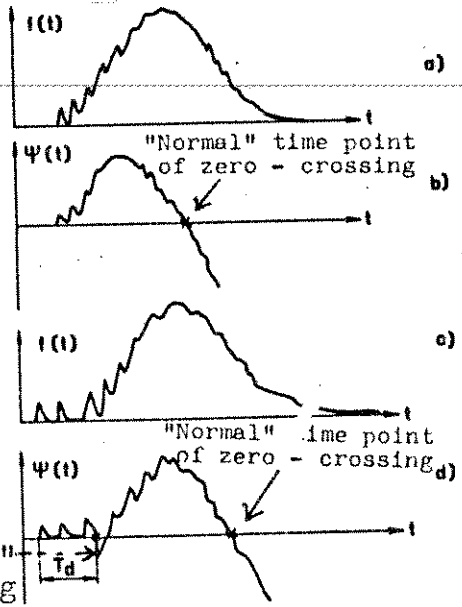


Fig.4 The same as at Fig. 3, 50+1000 PE, small filtration $F(f_{SER}$ width divided by half-width of the laser pulse)

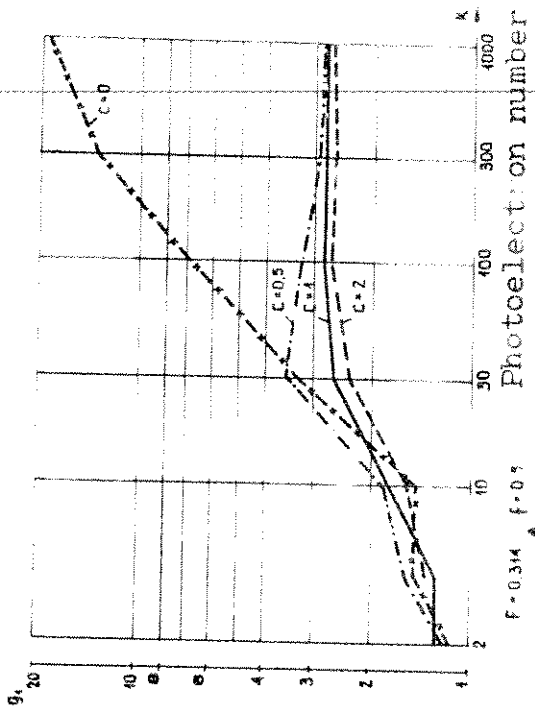


Fig. 6a

Fig. 6b

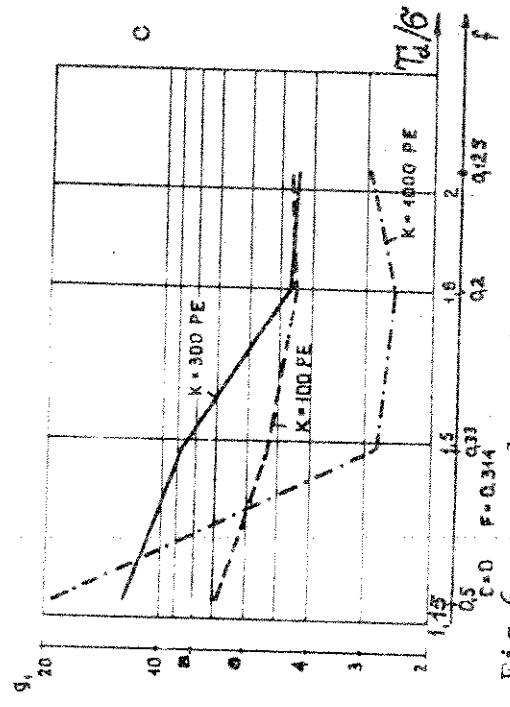
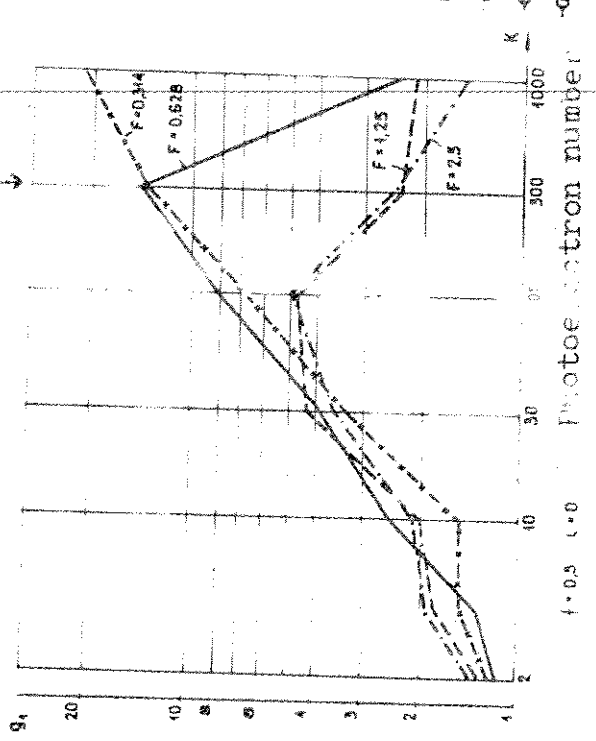


Fig. 6. g_1 values obtained from simul. a/ vs energy and charge sensitivity, b/ vs energy and filtration, c/ vs energy and normalised delay $T_d/6$ (fraction value changes also)

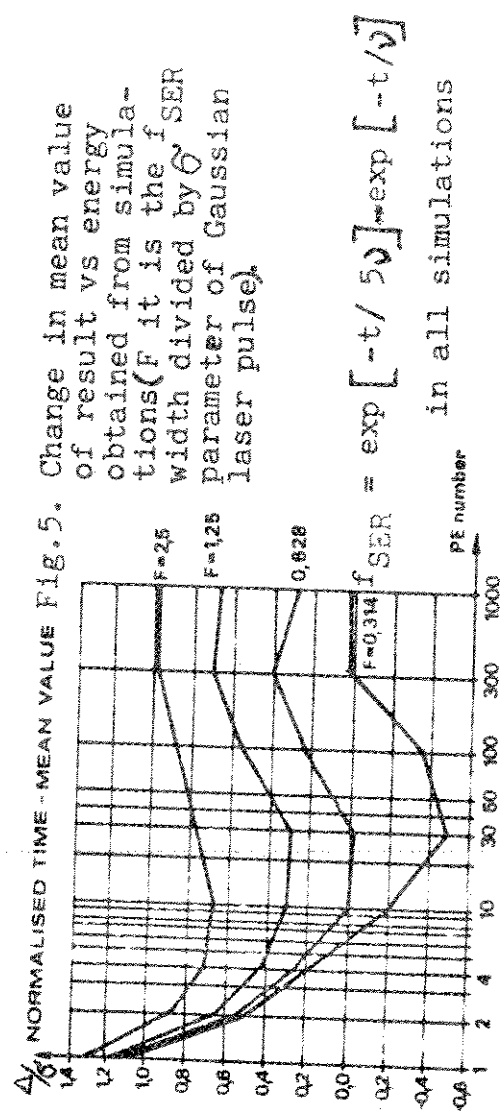


Fig. 5. Change in mean value of result vs energy obtained from simulations (F it is the f_{SER} width divided by σ_{SER} parameter of Gaussian laser pulse).

$$f_{SER} = \exp[-t/50] \exp[-t/v]$$

in all simulations

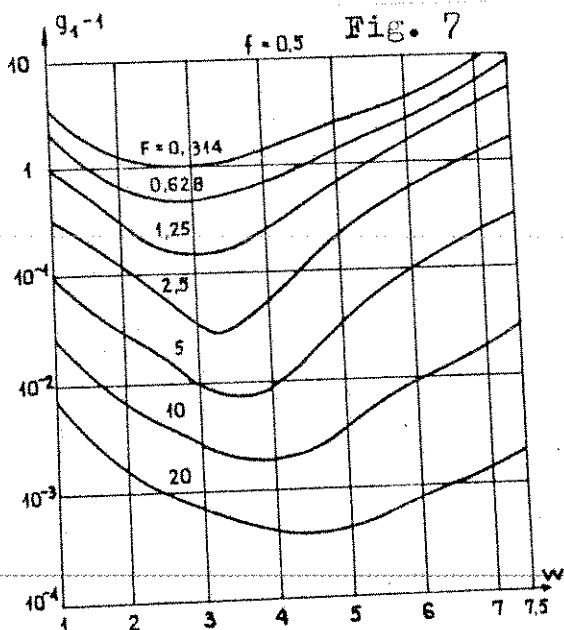
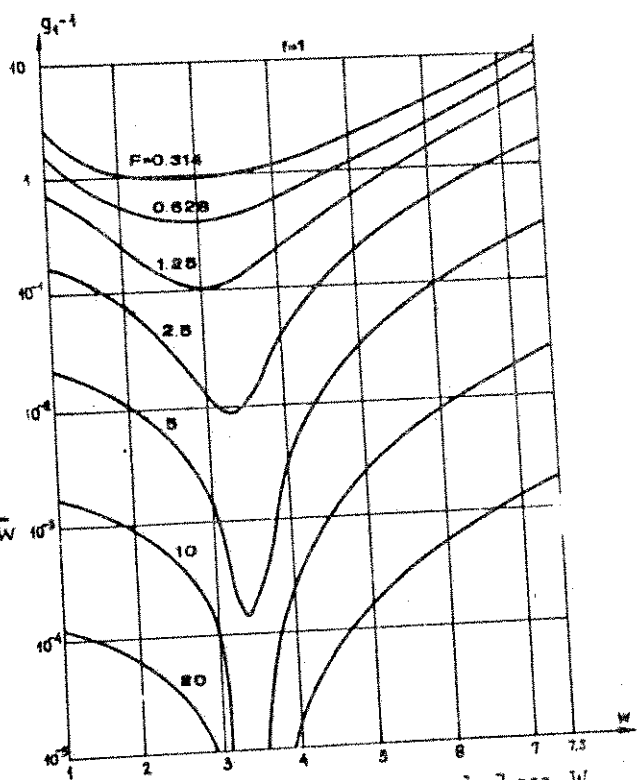
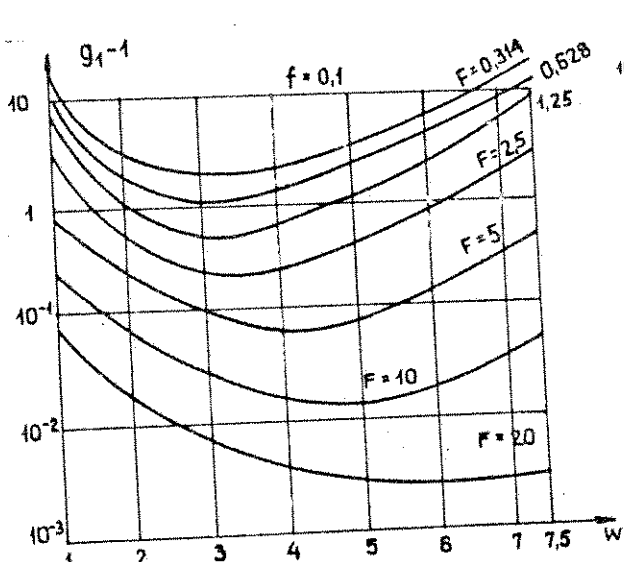


Fig. 7. g_1-1 values vs delay W and filtration F for 3 values of fraction f .

Fig. 7

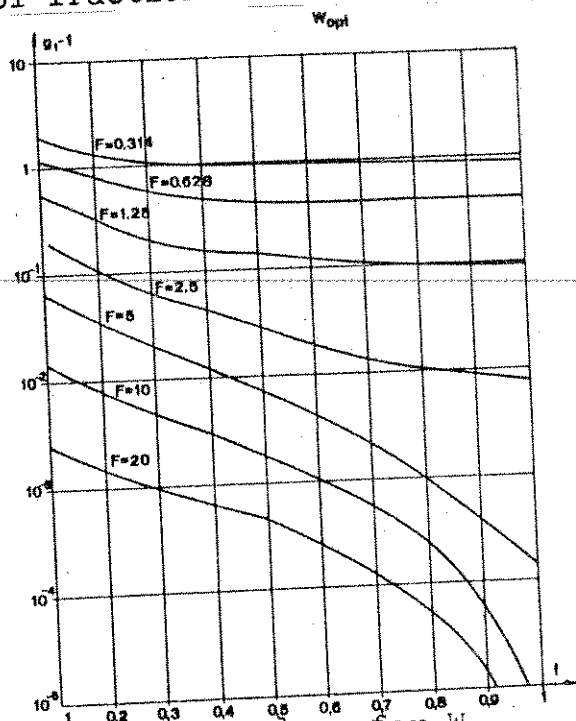


Fig. 9. g_1-1 values for W_{opt} vs fraction f and filtration F

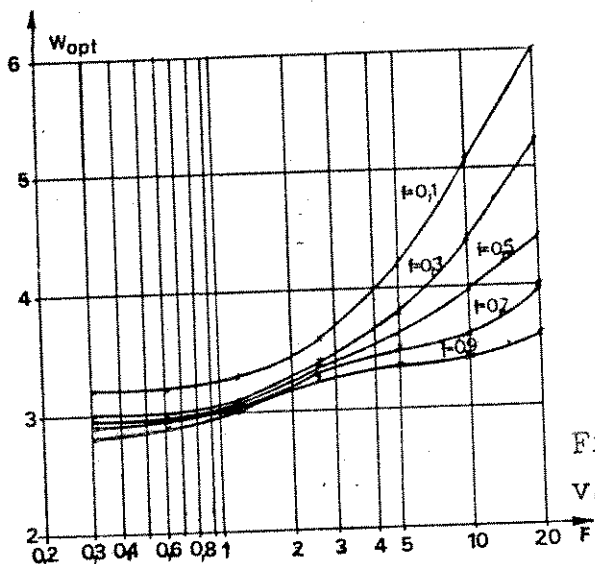


Fig. 8. Optimum delay W_{opt} values vs filtration F and fraction f .

CALIBRATION OF SUB-PICOSECOND TIMING SYSTEMS

B.A. Greene
Division of National Mapping
P.O. Box 31
Belconnen ACT 2616 - Australia -

Telephone (6162) 525095
Telex AA 62230

ABSTRACT

The difficulties of calibrating picosecond precision timing systems are discussed. A wide range of techniques are considered, and a minimum configuration for rigorous calibration is described. High speed techniques that lend themselves to full automation are evaluated in the context of a fully operational system.

CALIBRATION OF SUB-PICOSECOND TIMING SYSTEMS

B.A. Greene

1. Introduction

The recent development of timing systems with picosecond and even sub-picosecond accuracy has stimulated a requirement to calibrate such systems. In SLR systems the systematic errors are of overriding importance, and even if real time surveillance of the absolute accuracy [1] of the SLR system as a whole is maintained, it is still essential to be able to calibrate the timing sub-system independently. Once calibrated, it is a tool which can then be used to characterise the errors, systematic and otherwise, in other sub-systems.

The principal requirements for timing system calibration are to establish

- . stability
- . continuity ('smoothness')
- . linearity

If these characteristics are properly established, then the absolute accuracy of the timing system is rigorously proven.

In the context of a time interval measurement system, stability can be defined as the RMS error associated with a straight line fit of zero slope against time for a constant (not necessarily known) time interval.

Linearity is defined as the degree to which system error is proportional to length of time interval measured.

Continuity is defined as the degree to which linearity and stability are maintained as the time interval between test (calibration) points is reduced continuously.

A rigorous calibration procedure must examine all of these parameters.

In this paper we discuss several calibration techniques, and the role they can play in establishing system accuracy in terms of which of the above criteria are adequately tested.

2. Delay Line Calibrations

An established calibration technique for nanosecond timing systems utilizes an array of switchable coaxial delay lines, which have been pre-measured and are thus of 'known' delay. Even if it is assumed that the original calibration of each delay line was accurate without limit, this technique is unsuitable for picosecond calibrations because

- cable ageing causes delay changes
- cable flexing causes delay changes
- typical switch repeatability is only 3 ps RMS
- cable delays are temperature dependent
- coaxial connect-reconnect repeatability is only 3 ps RMS

This technique can be adapted to produce sub-picosecond tests of stability only. If the cable temperature is controlled such that the delay is stable to 0.5 ps RMS, then long term stability tests can be conducted on the timing system. A typical temperature sensitivity for coaxial cable is 0.03% per degree (C). Although temperature servos have been developed which can offer .001°C temperature control, it is in practice difficult to control coaxial cable to better than 0.1°C for each 50 ns of delay. That is, 0.5 ps stability can be readily obtained up to about 17 ns of delay. This is of little use if time interval units (TIUs) are used directly (i.e. in time interval mode) to measure satellite range. However, if precision TIU's are used as the high precision vernier of an epoch timing system, it is not necessary for them to count beyond 20 ns. Thus temperature stabilised delay lines can be used for 0.5 ps stability tests throughout the range of use of the TIU.

3. Variable Delay Lines

Rigid coaxial delay lines have been manufactured for calibrating the linearity and continuity of timing systems. These systems proliferated during a period when 100 ps timing system accuracy was the achievable limit, and could be expected to be inadequate for picosecond calibrations. This is the case, although some well constructed variable (rigid) coaxial delays can produce 3 ps RMS linearity and repeatability. Their stability will depend on delay length chosen, heat sources and sinks attached to the delay, and mechanical wear.

4. Dual Oscillator Techniques

It is now possible to obtain crystal oscillators which have sub-picosecond stability over 1 second, and ageing rates which are undetectable over 20 minutes with present instrumentation. The relative phase of two such oscillators provides a very slowly and linearly time varying delay for calibration purposes. This calibration technique is in everyday use at some SLR sites [2,3], using less stable oscillators for coarser (50 ps) calibrations. Provided that care is taken in generating the pulses to the timing system from the crystal output frequencies, this technique can give 1 ps linearity and accuracy, and sub-picosecond continuity checks.

5. Phase Locked Loop Method

An alternative oscillator phase technique utilises a single high stability oscillator and another oscillator phase-locked to it. The phase angle is programmable allowing selection of the relative phase of the crystals and thus a time interval. This technique gives linearity and continuity test capability, but is inherently noisier than the dual oscillator technique (above).

The noise attributable to the phase locking process can be brought down to around 5 ps if great care is taken with the circuit design. In addition, several picoseconds of systematic error arise from non-linearities in state-of-the-art phase angle programming circuits.

6. Optical Delay Line (ODL)

The time required for light to travel up to 10 m in air is virtually independent of environmental parameters [4]. To effect a 0.5 ps change in observed optical delay, environmental changes of the following order would be required:

$$\begin{array}{l} P = 30 \text{ mb} \\ \text{or} \\ P_w = 200 \text{ mb} \\ \text{or} \\ T = 10^\circ\text{C} \end{array}$$

[where P is atmospheric pressure, P_w is water vapour pressure, and T is air temperature]

The use of an optical delay line provides excellent linearity, accuracy, continuity, and stability. For example, if the delay elements are used to form a one-way light path, 100 microns of displacement of either end will cause a 0.33 ps change in the delay. Since the delay path can be very accurately controlled, to within a few microns, femtosecond resolution and accuracy can be obtained for differential delays.

For a two-way (folded path) calibration range, only 1.5 m of travel is required to produce a delay change of 10 ns. Such a path length is both simple to control environmentally and quite simple to automate for translation with 0.1 mm accuracy. Thus high resolution verniers with up to 10 ns full scale count can be absolutely calibrated to 0.66 ps under program control.

The technique is usually limited by the characteristics of the optical transmitter and receiver used to generate and detect the light pulse which transmits the delay so accurately formed. Using a 30 ps FWHM diode laser transmitter, and a 30 ps risetime detector, sub-picosecond relative accuracy, stability, and resolution can be achieved, provided environmental parameters are controlled.

7. Ensemble Techniques

The process of refining the accurate determination of time interval is analogous to that of defining time itself. The well established technique of using clock ensembles and optimised algorithms for manufacturing a timescale can be readily adapted to the time interval problem.

The use of as large an ensemble as possible of time interval counters is suggested by two factors arising from a very limited development program for TIUs for the Natmap Laser Ranging System (NLRS) at Orroral:

- no single TIU was ever constructed or tested which had better than 8 ps RMS single-estimate uncertainty for time interval.
- even the very best units ever tested at Orroral would exhibit occasional and inexplicable short term (minute) systematic excursions of up to 4 standard errors of a single estimate as measured from the long term average. Over a long period (20 mins) these units would produce sub-picosecond (averaged) stability of a mean estimate.

Since the Orroral program goal was to produce 5 ps RMS single estimate random errors with 0.5 ps systematic error, it was necessary to aggregate the performance of many TIUs to damp out excursions and to statistically reduce time interval errors.

A feature of the ensemble technique is that it requires very compact TIU design, so that a large number of TIUs can be fed an electronic signal over short paths, and so that complete environmental control of the ensemble is possible.

It has been found that the ensemble techniques are very effective in improving the resolution and linearity of TIU systems. Ensemble techniques do not yield absolute accuracy, but do facilitate absolute accuracy calibration of systems by improving linearity. The decay of accuracy of an ensemble is also significantly slower than that of individual TIUs, allowing less frequent resort to absolute accuracy calibrations, which can be tedious to execute rigorously.

The ensemble techniques can be used to calibrate individual TIUs simply by examining the performance of the unit in comparison to the ensemble mean. In general, if the ensemble is well behaved, errors in the individual TIUs can be readily identified. The technique lends itself very well for total automation, but is clearly not rigorous.

8. Calibration Techniques for the NLRS

Although the NLRS has the capability to apply any of the above calibration techniques, in practice the only techniques routinely used are:

- optical delay line
- fixed (stable) cable delays
- ensemble

The NLRS is constrained to operate almost totally automated. Thus only techniques which can lend themselves to total automation can be routinely used. The optical delay line method, which is the only rigorous technique listed above, is used very infrequently because it is not totally automated (here defined as requiring no user intervention whatsoever).

The timing system philosophy for the NLRS uses a large ensemble to reduce random error and give momentum to the system (the ensemble characteristics change more slowly than those of its elements). These ensembles can then be monitored very infrequently using a primary (rigorous) test such as ODL.

Such a complex calibration technique is not required to monitor the ensembles for accuracy. In practice a very simple approach is used, called fixed delay epoch measurement (FDEM).

For FDEM, two electronic pulses are obtained from a fixed, stable, delay cable built into the timing system. One NLRS timing ensemble measures the epoch of the first pulse, whilst a second ensemble measures the epoch of the second. The pulses are sourced such that they are totally random in phase with respect to the time base of the epoch timing system. Thus the full count range of the ensembles will be sampled if many measurements are taken. The delay is obtained by subtracting epochs. An error in either ensemble, at any point in its range, will cause the distribution of delay estimates to depart from the ideal. This is most easily seen as an increase in the spread of the distribution.

Because the delay is fixed, the error space of the ensemble measuring the second epoch is not sampled randomly. That is, the point in its range which is sampled is 100% correlated with the sample point of the first ensemble. Thus it is possible for errors to compensate and go undetected. The probability of this is reduced significantly if more than one delay is used.

The utility of this technique, which is used before every tracking operation, has been borne out by occasional applications of rigorous tests such as ODL.

The three techniques in routine use at Orroal are thus applied in the following way:

- (a) On every shot. On each shot, at least 34 estimates of epoch are made. The ensemble size is large enough to give a good reduction in systematic drift and random error over individual TIU elements. Individual TIU readings are processed through a double-pass filter which utilises the recent performance history of a TIU to adjust its reading before comparing it to the ensemble mean in the filter process. Units may be 'accepted' or 'rejected'. Consistent rejection implies a need for repair or recalibration.

Also on each shot, a real-time calibration of system delay is made. This is essentially an ODL calibration in which the delay is not known a priori to better than 200 ps, because of long term drift in the apparatus. However, the system delay so measured can be and is used in an FDEM sense. The calibration curve is displayed, shot by shot, in real time, with picosecond resolution, so that the operator (if present) can monitor the overall system performance, including timing. The data is continuously analysed in real time, and statistics presented to the operator. Only gross errors of over 40 ps would be detected at this stage because the detector used (MCP-PMT) has around 40 ps RMS error itself, and can walk 40 ps during a typical SLR pass.

- (b) Before each pass.

Before each pass, over 3000 samples of timing system performance are taken in FDEM mode, under total software control. The FDEM algorithm in use calculates the signal delays to each ensemble, and trims them into equality before the pass commences (usually only a few ps adjustment).

- (c) Occasionally the granularity and accuracy of the timing system are checked independently. A good test for continuity of the timing system is obtained by taking a delay line and heating it for 1 minute and then allowing it to cool. The thermal relaxation produces a delay continuum. If the delay is sampled at 50 Hz, delay changes of 20 fs can be sampled. Figure 1 shows a typical result from a continuum test of this kind, showing individual delay measurements. Strong structure at the picosecond level is evident, but the results show very good performance overall.

The accuracy calibration used is the ODL technique, applied infrequently because of its need for operator intervention.

Finally, system stability checks are carried out periodically. A typical stability plot for the NLRS timing system is shown in Figure 2. Each point plotted is a normal point of 400 ensemble estimates of a fixed and stable delay. The RMS error of a straight line fit to the data shown is around 0.6 ps, which is a typical result. The suggestion of a cyclic systematic error is present in the data. This has been seen in ODL tests also, so it is likely to be attributable to the timing system.

9. Comments

The electronic measurement of time interval to the picosecond level is exceedingly complex. The NLRS timing system can only approach picosecond performance on a statistical basis. That is, it is beyond our present technology to adjust a delay by 5 picoseconds and be 100% confident that the TIU single sample reading, or even that of a TIU ensemble, will change by 5 picoseconds. However, if many hundreds of estimates are made, delay changes of less than 1 ps can be accurately determined by TIU ensembles.

REFERENCES

1. Greene, B.A., "Calibration of Sub-Millimetre Precision Satellite Laser Ranging Systems", proc. Sixth International Workshop on Laser Ranging Instrumentation, to be published.
2. Sinclair, A., Royal Greenwich Observatory, UK, Private Communication.
3. Steggerda, C. University of Maryland, USA, Private Communication.
4. Owens, J.C., "Optical refractive index of air dependence on pressure temperature and composition", Appl. Opt., Vol 6, No 51, 1967.

Figure 1

TIMING CONTINUUM TEST

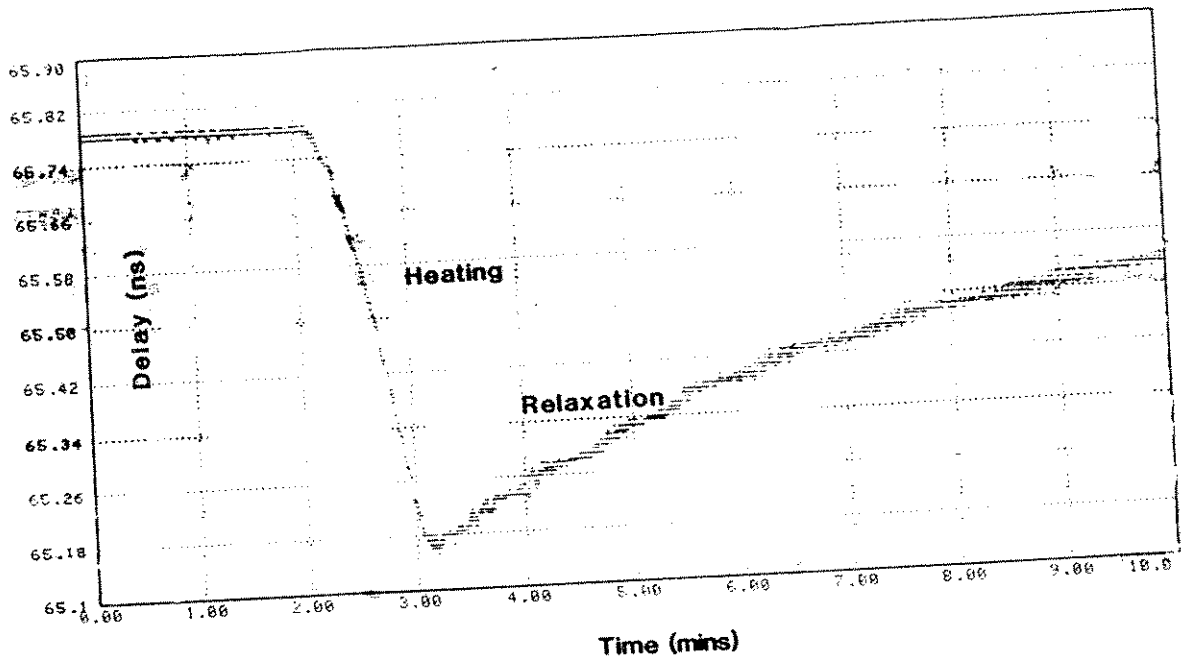
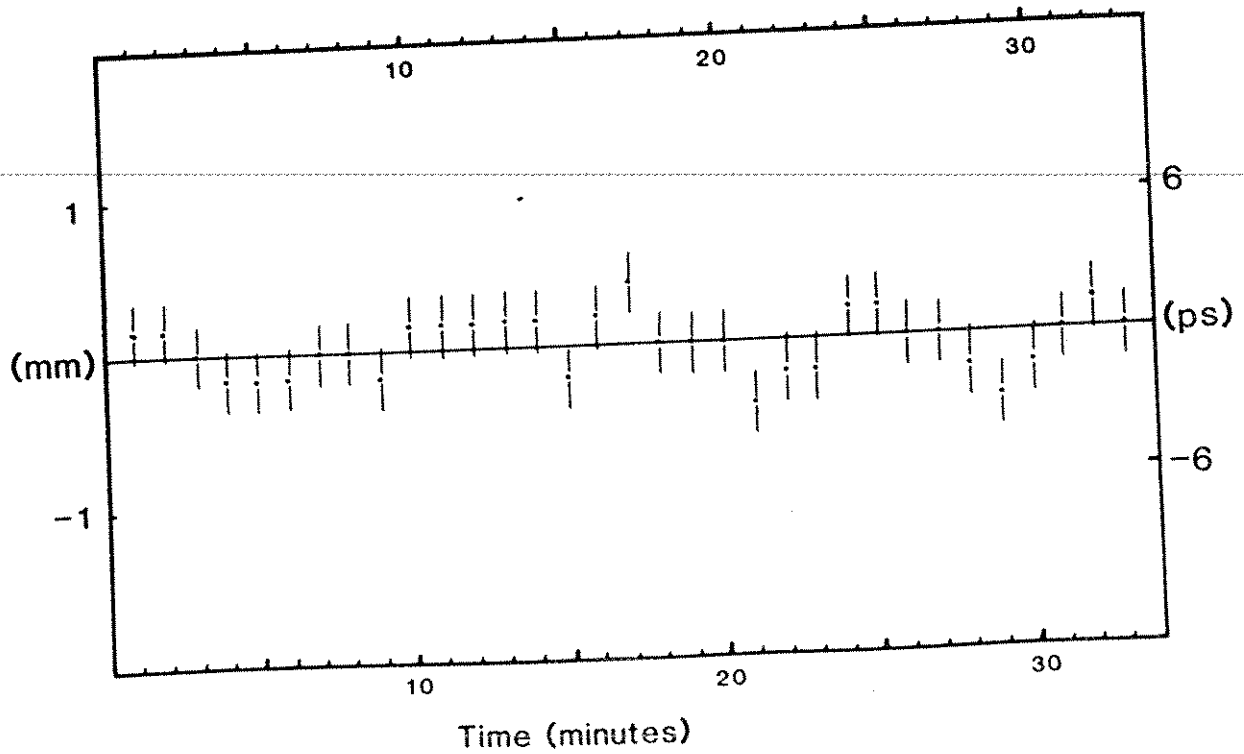


Figure 2

NLRS TIMING STABILITY



RECENT ADVANCES IN THE GLTN TIMING AND
FREQUENCY INSTRUMENTATION

P. DacheI, and Al
Bendix Field Engineering Corporation
One Bendix Road
Columbia, Maryland 21045 - USA -

Telephone (301) 964 7189
TWX 198120 BENFLD COLB

ABSTRACT

The stringent epoch time requirements necessary for the Goddard Laser Tracking Network to satisfy its global geodetic survey programs have consistently pushed the state of the art. As geophysical baseline accuracy requirements have approached the sub centimeter level, new time and frequency technologies have been sought.

This paper will describe the early Global Positioning Satellite (GPS) time transfer receiver development. The GPS receiver development program at the Naval Research Laboratory for NASA was the forerunner of many commercial efforts which have led to unitized construction and firmware controlled receivers. Along with the GPS receiver development, NASA worked with other U.S. and international timing organizations to develop strategies to optimize the use of these receivers by forming a global timing network for geophysical measurements. Through the use of "common look" techniques a laser tracking site may observe a GPS satellite simultaneously with the data reduction center which is in turn synchronized to UTC via USNO. Using this common look technique, orbital & spacecraft clock systematic errors may be minimized.

With a need for greater synchronization accuracy also grew the need for improved short term frequency stabilities. In the past, where less accurate geodetic measurements were being performed, much of the low level phase noise and frequency instabilities were seen as random processes. Recent investigation has shown that many of these frequency instabilities have systematic signatures which contribute to measurement error. To meet the sub centimeter accuracy goal of the Crustal Dynamics Program the need for picosecond short term stabilities in generation, distribution and monitoring systems is becoming a necessity. System options are described which will allow a spectrally pure crystal oscillator (better than 2 picoseconds over a 50 millisecond interval) to be frequency locked and steered to epoch time accuracies of 100 nanoseconds via the GPS system.

Prior to the inception of the Goddard Laser Tracking Network (GLTN) ten years ago, NASA required that satellite support stations be synchronized within ± 25 microseconds. The GLTN need for ± 1 microsecond world-wide time synchronization required the development of new methods for maintaining time synchronization.

Recognizing that conventional means of timekeeping using LORAN-C, HF and VLF could not practically achieve the required ± 1 microsecond global clock synchronization, the cesium portable clock was used to provide time synchronization. Periodic portable clock trips were made to each station to determine the station's nominal LORAN-C value. Each station's cesium clock offset from U.S. Naval Observatory (USNO) time was plotted from daily LORAN-C values, time steps were calculated to synchronize station time to USNO time, and the station was directed to make the proper equipment adjustments to achieve the recommended time step.

With the improvement of laser equipment and the demand for more accurate ranging, the need for sub-microsecond timing has become a valid requirement.

This need prompted investigation and development of satellite timing receivers in a combined effort between the Naval Research Laboratory and NASA.

The Navigational Technology Satellite receiver was developed as a forerunner to the GPS Time Transfer Receiver now being used for sub-microsecond time transfer.

GPS TIMING

Techniques are being developed to utilize GPS timing for the GLTN, with a goal of world-wide time synchronization to the greatest feasible accuracy.

To utilize the time transfer capability of the GPS, a timing receiver was developed by the Naval Research Laboratory (NRL) for NASA, was tested at field sites, and was used in time transfer experiments (References 1 and 2). The first commercial GPS time transfer receiver was built by Stanford Telecommunications Incorporated (STI). This receiver was evaluated for possible use in the GLTN. The STI and the NRL receivers are operated from a keyboard similar to that of a personal computer. The cost of the STI receiver was approximately one half that of the NRL receiver and it was more suitable for mobile installations. More recently a third receiver, the Frequency and Time Systems (FTS) Model 8400 was evaluated and found to be the best suited for GLTN operations because of its smaller size, unit construction and lower cost.

Figures 1 and 2 compare time transfer data obtained with an FTS 8400 GPS receiver or the identical Trimble 5000A and a cesium portable clock at several timing installations. Portable clock time was compared to USNO time before and after these trips. The measurements were supplemented by TV Line 10 measurements which were accurate to +/- 50 nanoseconds with respect to USNO.

Figure 3 lists current deployments of FTS 8400 GPS timing receivers in the GLTN.

GLTN GPS DATA COLLECTION

GPS time position measurements are made daily at the GLTN stations. The stations collect GPS data twice a day for each visible satellite. The raw time position reading is recorded during the 10-minute satellite observation pass. This data point along with the date, time, and satellite vehicle number are recorded for each measurement. The measurement data are transmitted to the NASA Communications Center in the daily Laser Operations Report (LOR). Also transmitted in the LOR is information concerning station time steps, frequency changes, power outages, equipment problems, etc.

AUTOMATED TIME POSITION SYSTEM (ATPS)

The Automated Time Position System is the means by which station time is monitored and analyzed for the GLTN. The ATPS

- o provides daily time position determination
- o calculates long term cesium frequency drift
- o predicts the date the station tolerances exceed 1 microsecond
- o evaluates the validity of data and data analysis methods

The System includes several computer programs that (1) read the LOR data into the ATPS data bases, (2) permit the manual entry, editing, deletion, and listing of data files and (3) perform the analysis of the timing measurements. The system is coded in FORTRAN and runs on a VAX computer

cluster. The cluster consists of two VAX-11/780 computers and one VAX 8600 computer. The analysis program is operator inactive and produces a printed data output. The data output consists of the source listing data from the data files used in the analysis, a least-squares calculation of the original source data, and a line printer graph of the original and least-squares data plot.

GPS COMMON VIEW

Utilizing the GPS common view technique described in Reference 3, orbital and spacecraft clock systematic errors can be minimized.

A common view/near common view GPS time transfer experiment was conducted in 1983 to determine the accuracy of GPS time transfer receivers for the GLTN (Reference 4). The experiment was conducted between the Bureau International de l'Heure (BIH), Paris, France, the Institute Fur Angewandte Geodasie (IFAG), Wettzel, Germany and the GLTN data reduction center at Columbia, Maryland. The local time bases incorporated HP5061 (Option 004) Cesium standards or hydrogen masers. Results of the experiment showed the overall accuracy to be consistently better than 100 nanoseconds. Recent improvements in the GPS system have permitted common view accuracies approaching 10 to 20 nanoseconds. (Reference 5).

Efforts are underway to utilize GPS common view techniques on a day-to-day operational basis in the GLTN (Figure 4).

TIME INTERVAL MEASUREMENT ERRORS

The GLTN utilizes Hewlett Packard 5370 time interval counters with an atomic standard for the time base. The 5370 has a 20 picosecond single shot resolution, however, the accuracy is typically +/- 40 picoseconds. The accuracy of the time interval measurement is influenced by the summation of:

- o trigger level
- o input signal noise
- o interval timing jitter
- o time base short term stability

Event timers developed by the University of Maryland and by the Division of National Mapping (Australia) reduce the internal timing jitter and improve the short term stability. The University of Maryland unit uses a 200 MHZ oscillator phase locked to the atomic standard.

IMPROVEMENTS IN SHORT TERM STABILITY

Improved short term stability oscillators that can be steered to UTC via the GPS are being developed.

Austron, Inc. and the GLTN are developing a low noise disciplined frequency standard (Reference 6) that utilizes a microprocessor controlled system which automatically locks the frequency of a precision BVA crystal oscillator to an atomic standard having superior long term stability.

With the use of a third-order servo technique, the instrument is able to correct the frequency offset and aging of the internal BVA oscillator. If the frequency of the atomic standard is altered (due to loss of lock, loss of signal or failure) the unit will continue to apply corrections to the internal BVA oscillator. These corrections are calculated from data accumulated while the atomic standard is stable. These corrections are automatic and do not disturb the phase. This technique minimizes the effect of aging of the BVA oscillator and holds the unit to within ± 3 parts in 10^{12} per day.

The short term stability (50 milliseconds to 100 seconds) of the low noise disciplined frequency standard is represented in Figure 5. The internal BVA oscillator has a short term stability σ ($\tau = 0.2$ to 30 seconds) $\approx 5 \times 10^{-13}$ and an aging rate of 1×10^{-11} per day. Frequency steering of the low noise disciplined oscillator by the atomic standard to epoch time accuracies of 100 nanoseconds via the GPS system can be achieved.

REFERENCES

1. J. Oaks, J. Buisson, C. Wardrip, "GPS Time Transfer Receivers for the NASA Transportable Laser Ranging Network", NASA/GSFC x-814-82-6, April, 1982.
2. J. Oaks, A. Franks, S. Falvey, M. Lister, J. Buisson, S. Wardrip and H. Warren, "Prototype Design and Initial Test Evaluation of a GPS Time Transfer Receiver", NRL report 8608, July 27, 1982.
3. D. W. Allan and M. A. Weiss, "Accurate Time and Frequency Transfer during Common-View of a GPS Satellite", Proceedings of 34th Annual Frequency Control Symposium, 1980.
4. C. Wardrip, J. Buisson, J. Oaks, et al., "An International Time Transfer Experiment", Proceedings of the 37th Annual Frequency Control Symposium, 1983.
5. M. A. Weiss, "Weighting and Smoothing of Data in GPS Common View Time Transfer", Proceedings of the 17th Annual Precise Time and Time Interval Applications and Planning Meeting, 1985.
6. B. Bourke and B. Penrod, "An Analysis of a Microprocessor Controlled Disciplined Frequency Standard", Proceedings of the 37th Annual Frequency Control Symposium, 1983.

<u>FEB 5 1985</u>	<u>MOBLAS 1 TAHITI</u>	<u>GPS SV</u>	<u>PC VS USNO USING GPS</u>	<u>PC VS USNO CALCULATED</u>	<u>(GPS-USNO) - (PC-USNO)</u>
		06	2.003	1.991	+0.012 *
		08	1.996	1.991	+0.005
		09	2.009	1.991	+0.018
		11	2.012	1.991	+0.021
		13	1.999	1.994	+0.005
		12	1.995	1.997	-0.002

ALL VALUES IN MICROSECONDS

TIMES VERIFIED BY PORTABLE CLOCK CLOSURES WITH USNO.

* ±200 NANOSECONDS DUE TO SATELLITE AND PORTABLE CLOCK ERRORS.

FIGURE 1 - GPS VS PORTABLE CLOCK TIME TRANSFER.

<u>STATION</u>	<u>DATE OF INSTALLATION</u>
MOBLAS-2 ISRAEL	SEPTEMBER 85
MOBLAS-5 WESTERN AUSTRALIA	OCTOBER 85
MOBLAS-6 MEXICO	MAY 86
HOLLAS HAWAII	APRIL 86
SAO-2 PERU	AUGUST 86
NATMAP AUSTRALIA	OCTOBER 85
MLRS TEXAS	JUNE 86
TLRS-1 GORF	NOVEMBER 85
TLRS-2 GORF	NOVEMBER 85
MATERA	NOVEMBER 86 (PROPOSED)

FIGURE 3 - DEPLOYMENT OF FTS-8400 GPS TIME TRANSFER MONITORS

<u>DATE</u>	<u>LOCATION</u>	<u>(PC VS USNO) USING GPS</u>	<u>(PC VS USNO) CALCULATED</u>	<u>(GPS-USNO) - (PC-USNO)</u>
FEB 12 1985	CSIRO, AUSTRALIA	2.087	1.989	0.098*
FEB 13 1985	NATMAP, AUSTRALIA	2.050	2.030	0.020
FEB 14 1985	TIDBINBILLA, AUSTRALIA	2.160	2.068	0.092
FEB 16 1985	MOBLAS 5, AUSTRALIA	2.243	2.159	0.084
FEB 19 1985	TELCOM, AUSTRALIA	2.262	2.262	0.000
FEB 20 1985	CSIRO, AUSTRALIA	2.275	2.296	-0.021
FEB 22 1985	HOLLAS, HAWAII	2.395	2.406	-0.011

ALL VALUES IN MICROSECONDS

USNO CLOSURE ON FEB 8 AND FEB 27, 1985

* ±200 NANoseconds DUE TO SATELLITE AND PORTABLE CLOCK ERRORS.

FIGURE 2 - GPS VS PORTABLE CLOCK TIME TRANSFER

FREQUENCY COMPARISON OF VARIOUS STANDARDS

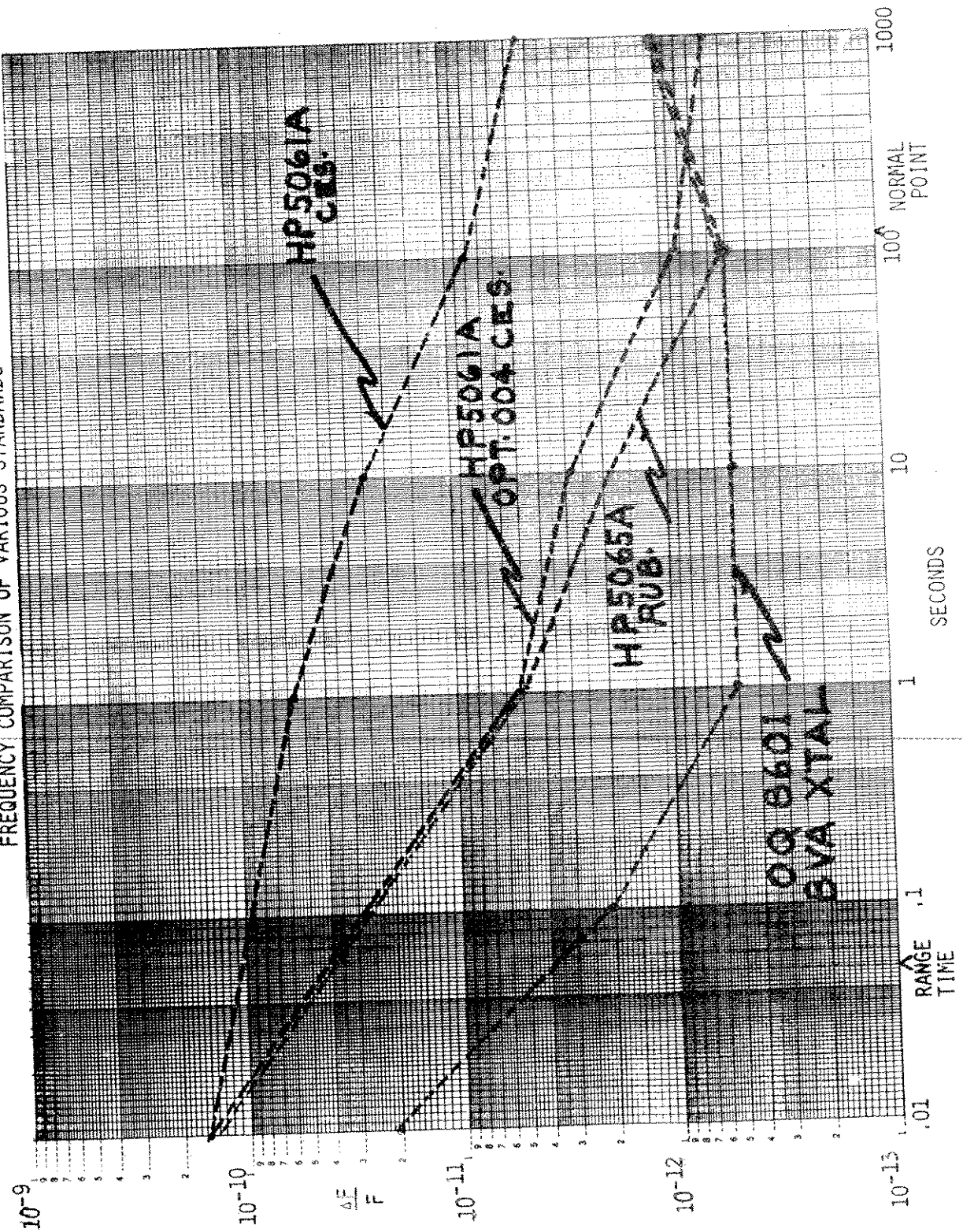


FIGURE 5

Prior to the inception of the Goddard Laser Tracking Network (GLTN) ten years ago, NASA required that satellite support stations be synchronized within ± 25 microseconds. The GLTN need for ± 1 microsecond world-wide time synchronization required the development of new methods for maintaining time synchronization.

Recognizing that conventional means of timekeeping using LORAN-C, HF and VLF could not practically achieve the required ± 1 microsecond global clock synchronization, the cesium portable clock was used to provide time synchronization. Periodic portable clock trips were made to each station to determine the station's nominal LORAN-C value. Each station's cesium clock offset from U.S. Naval Observatory (USNO) time was plotted from daily LORAN-C values, time steps were calculated to synchronize station time to USNO time, and the station was directed to make the proper equipment adjustments to achieve the recommended time step.

With the improvement of laser equipment and the demand for more accurate ranging, the need for sub-microsecond timing has become a valid requirement.

This need prompted investigation and development of satellite timing receivers in a combined effort between the Naval Research Laboratory and NASA.

The Navigational Technology Satellite receiver was developed as a forerunner to the GPS Time Transfer Receiver now being used for sub-microsecond time transfer.

GPS TIMING

Techniques are being developed to utilize GPS timing for the GLTN, with a goal of world-wide time synchronization to the greatest feasible accuracy.

To utilize the time transfer capability of the GPS, a timing receiver was developed by the Naval Research Laboratory (NRL) for NASA, was tested at field sites, and was used in time transfer experiments (References 1 and 2). The first commercial GPS time transfer receiver was built by Stanford Telecommunications Incorporated (STI). This receiver was evaluated for possible use in the GLTN. The STI and the NRL receivers are operated from a keyboard similar to that of a personal computer. The cost of the STI receiver was approximately one half that of the NRL receiver and it was more suitable for mobile installations. More recently a third receiver, the Frequency and Time Systems (FTS) Model 8400 was evaluated and found to be the best suited for GLTN operations because of its smaller size, unit construction and lower cost.

Figures 1 and 2 compare time transfer data obtained with an FTS 8400 GPS receiver or the identical Trimble 5000A and a cesium portable clock at several timing installations. Portable clock time was compared to USNO time before and after these trips. The measurements were supplemented by TV Line 10 measurements which were accurate to ± 50 nanoseconds with respect to USNO.

Figure 3 lists current deployments of FTS 8400 GPS timing receivers in the GLTN.

GLTN GPS DATA COLLECTION

GPS time position measurements are made daily at the GLTN stations. The stations collect GPS data twice a day for each visible satellite. The raw time position reading is recorded during the 10-minute satellite observation pass. This data point along with the date, time, and satellite vehicle number are recorded for each measurement. The measurement data are transmitted to the NASA Communications Center in the daily Laser Operations Report (LOR). Also transmitted in the LOR is information concerning station time steps, frequency changes, power outages, equipment problems, etc.

AUTOMATED TIME POSITION SYSTEM (ATPS)

The Automated Time Position System is the means by which station time is monitored and analyzed for the GLTN. The ATPS

- o provides daily time position determination
- o calculates long term cesium frequency drift
- o predicts the date the station tolerances exceed 1 microsecond
- o evaluates the validity of data and data analysis methods

The System includes several computer programs that (1) read the LOR data into the ATPS data bases, (2) permit the manual entry, editing, deletion, and listing of data files and (3) perform the analysis of the timing measurements. The system is coded in FORTRAN and runs on a VAX computer cluster. The cluster consists of two VAX-11/780 computers and one VAX 8600 computer. The analysis program is operator inactive and produces a printed data output. The data output consists of the source listing data from the data files used in the analysis, a least-squares calculation of the original source data, and a line printer graph of the original and least-squares data plot.

GPS COMMON VIEW

Utilizing the GPS common view technique described in Reference 3, orbital and spacecraft clock systematic errors can be minimized.

A common view/near common view GPS time transfer experiment was conducted in 1983 to determine the accuracy of GPS time transfer receivers for the GLTN (Reference 4). The experiment was conducted between the Bureau International de l'Heure (BIH), Paris, France, the Institute Fur Angewandte Geodasie (IFAG), Wettzel, Germany and the GLTN data reduction center at Columbia, Maryland. The local time bases incorporated HP5061 (Option 004) Cesium standards or hydrogen masers. Results of the experiment showed the overall accuracy to be consistently better than 100 nanoseconds. Recent improvements in the GPS system have permitted common view accuracies approaching 10 to 20 nanoseconds. (Reference 5).

Efforts are underway to utilize GPS common view techniques on a day-to-day operational basis in the GLTN (Figure 4).

TIME INTERVAL MEASUREMENT ERRORS

The GLTN utilizes Hewlett Packard 5370 time interval counters with an atomic standard for the time base. The 5370 has a 20 picosecond single shot resolution, however, the accuracy is typically +/- 40 picoseconds. The accuracy of the time interval measurement is influenced by the summation of:

- o trigger level
- o input signal noise
- o interval timing jitter
- o time base short term stability

Event timers developed by the University of Maryland and by the Division of National Mapping (Australia) reduce the internal timing jitter and improve the short term stability. The University of Maryland unit uses a 200 MHz oscillator phase locked to the atomic standard.

IMPROVEMENTS IN SHORT TERM STABILITY

Improved short term stability oscillators that can be steered to UTC via the GPS are being developed.

Austron, Inc. and the GLTN are developing a low noise disciplined frequency standard (Reference 6) that utilizes a microprocessor controlled system which automatically locks the frequency of a precision BVA crystal oscillator to an atomic standard having superior long term stability. With the use of a third-order servo technique, the instrument is able to correct the frequency offset and aging of the internal BVA oscillator. If the frequency of the atomic standard is altered (due to loss of lock, loss of signal or failure) the unit will continue to apply corrections to the internal BVA oscillator. These corrections are calculated from data accumulated while the atomic standard is stable. These corrections are automatic and do not disturb the phase. This technique minimizes the effect of aging of the BVA oscillator and holds the unit to within +/- 3 parts in 10^{12} per day.

The short term stability (50 milliseconds to 100 seconds) of the low noise disciplined frequency standard is represented in Figure 5. The internal BVA oscillator has a short term stability σ ($\tau = 0.2$ to 30 seconds) $\approx 5 \times 10^{-13}$ and an aging rate of 1×10^{-11} per day. Frequency steering of the low noise disciplined oscillator by the atomic standard to epoch time accuracies of 100 nanoseconds via the GPS system can be achieved.

REFERENCES

1. J. Oaks, J. Buisson, C. Wardrip, "GPS Time Transfer Receivers for the NASA Transportable Laser Ranging Network", NASA/GSFC x-814-82-6, April, 1982.
2. J. Oaks, A. Franks, S. Falvey, M. Lister, J. Buisson, S. Wardrip and H. Warren, "Prototype Design and Initial Test Evaluation of a GPS Time Transfer Receiver", NRL report 8608, July 27, 1982.
3. D. W. Allan and M. A. Weiss, "Accurate Time and Frequency Transfer during Common-View of a GPS Satellite", Proceedings of 34th Annual Frequency Control Symposium, 1980.
4. C. Wardrip, J. Buisson, J. Oaks, et al., "An International Time Transfer Experiment", Proceedings of the 37th Annual Frequency Control Symposium, 1983.
5. M. A. Weiss, "Weighting and Smoothing of Data in GPS Common View Time Transfer", Proceedings of the 17th Annual Precise Time and Time Interval Applications and Planning Meeting, 1985.
6. B. Bourke and B. Penrod, "An Analysis of a Microprocessor Controlled Disciplined Frequency Standard", Proceedings of the 37th Annual Frequency Control Symposium, 1983.

